

Spectral Clustering Based on Local PCA

Ery Arias-Castro^{*1}, Gilad Lerman² and Teng Zhang³

We propose a spectral clustering method based on local principal components analysis (PCA). After performing local PCA in selected neighborhoods, the algorithm builds a nearest neighbor graph weighted according to a discrepancy between the principal subspaces in the neighborhoods, and then applies spectral clustering. As opposed to standard spectral methods based solely on pairwise distances between points, our algorithm is able to resolve intersections. We establish theoretical guarantees for simpler variants within a prototypical mathematical framework for multi-manifold clustering, and evaluate our algorithm on various simulated data sets.

Keywords: multi-manifold clustering, spectral clustering, local principal component analysis, intersecting clusters.

1 Introduction

The task of multi-manifold clustering, where the data are assumed to be located near surfaces embedded in Euclidean space, is relevant in a variety of applications. In cosmology, it arises as the extraction of galaxy clusters in the form of filaments (curves) and walls (surfaces) (Martínez and Saar, 2002; Valdarnini, 2001); in motion segmentation, moving objects tracked along different views form affine or algebraic surfaces (Chen et al., 2009; Fu et al., 2005; Ma et al., 2008; Vidal and Ma, 2006); this is also true in face recognition, in the context of images of faces in fixed pose under varying illumination conditions (Basri and Jacobs, 2003; Epstein et al., 1995; Ho et al., 2003).

We consider a stylized setting where the underlying surfaces are nonparametric in nature, with a particular emphasis on situations where the surfaces intersect. Specifically, we assume the surfaces are smooth, for otherwise the notion of continuation is potentially ill-posed. For example, without smoothness assumptions, an L-shaped cluster is indistinguishable from the union of two line-segments meeting at right angle.

Spectral methods (Luxburg, 2007) are particularly suited for nonparametric settings, where the underlying clusters are usually far from convex, making standard methods like K-means irrelevant. However, a drawback of standard spectral approaches such as the well-known variation of Ng, Jordan, and Weiss (2002) is their inability to separate intersecting clusters. Indeed, consider the simplest situation where two straight clusters intersect at right angle, pictured in Figure 1 below. The algorithm of Ng et al. (2002) is based on pairwise affinities that are decreasing in the distances between data points, making it insensitive to smoothness and, therefore, intersections. And indeed, this algorithm typically fails to separate intersecting clusters, even in the easiest setting of Figure 1.

As argued in (Agarwal et al., 2006, 2005; Shashua et al., 2006), a multiway affinity is needed to capture complex structure in data (here, smoothness) beyond proximity attributes. For example, Chen and Lerman (2009b) use a flatness affinity in the context of *hybrid linear modeling*, where the surfaces are assumed to be affine subspaces, and subsequently extended to algebraic surfaces via the ‘kernel trick’ (Chen, Atev, and Lerman, 2009). Moving beyond parametric models, Arias-Castro, Chen, and Lerman (2011) consider a localized measure of flatness; see also Elhamifar and Vidal (2011). Continuing this line of work, we suggest a spectral clustering method based on the

*Corresponding author: math.ucsd.edu/~eariasca

¹University of California, San Diego

²University of Minnesota, Twin Cities

³Institute for Mathematics and its Applications (IMA)

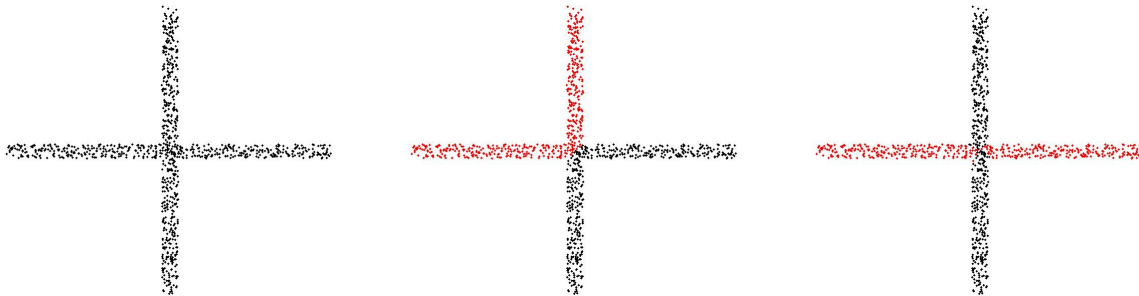


Figure 1: Two rectangular clusters intersecting at right angle. Left: the original data. Center: a typical output of the standard spectral clustering method of [Ng et al. \(2002\)](#), which is generally unable to resolve intersections. Right: our method.

estimation of the local linear structure (tangent bundle) via local principal component analysis (PCA).

The idea of using local PCA combined with spectral clustering has precedents in the literature. In particular, our method is inspired by the work of [Goldberg, Zhu, Singh, Xu, and Nowak \(2009\)](#), where the authors develop a spectral clustering method within a semi-supervised learning framework. Local PCA is also used in the multiscale, spectral-flavored algorithm of [Kushnir, Galun, and Brandt \(2006\)](#). This approach is in the zeitgeist. While writing this paper, we became aware of two very recent publications, by [Wang, Jiang, Wu, and Zhou \(2011\)](#) and by [Gong, Zhao, and Medioni \(2012\)](#), both proposing approaches very similar to ours. We comment on these spectral methods in more detail later on.

The basic proposition of local PCA combined with spectral clustering has two main stages. The first one forms an affinity between a pair of data points that takes into account both their Euclidean distance and a measure of discrepancy between their tangent spaces. Each tangent space is estimated by PCA in a local neighborhood around each point. The second stage applies standard spectral clustering with this affinity. As a reality check, this relatively simple algorithm succeeds at separating the straight clusters in [Figure 1](#). We tested our algorithm in more elaborate settings, some of them described in [Section 4](#).

Besides spectral-type approaches to multi-manifold clustering, other methods appear in the literature. The methods we know of either assume that the different surfaces do not intersect ([Polito and Perona, 2001](#)), or that the intersecting surfaces have different intrinsic dimension or density ([Gionis et al., 2005](#); [Haro et al., 2007](#)). The few exceptions tend to propose very complex methods that promise to be challenging to analyze ([Guo et al., 2007](#); [Souvenir and Pless, 2005](#)).

Our contribution is the design and detailed study of a prototypical spectral clustering algorithm based on local PCA, tailored to settings where the underlying clusters come from sampling in the vicinity of smooth surfaces that may intersect. We endeavored to simplify the algorithm as much as possible without sacrificing performance. We provide theoretical results for simpler variants within a standard mathematical framework for multi-manifold clustering. To our knowledge, these are the first mathematically backed successes at the task of resolving intersections in the context of multi-manifold clustering, with the exception of ([Arias-Castro et al., 2011](#)), where the corresponding algorithm is shown to succeed at identifying intersecting curves. The salient features of that algorithm are illustrated via numerical experiments.

The rest of the paper is organized as follows. In [Section 2](#), we introduce our methods. In [Sec-](#)

tion 3, we analyze our methods in a standard mathematical framework for multi-manifold learning. In Section 4, we perform some numerical experiments illustrating several features of our algorithm. In Section 5, we discuss possible extensions.

2 The methodology

We introduce our algorithm and simpler variants that are later analyzed in a mathematical framework. We start with some review of the literature, zooming in on the most closely related publications.

2.1 Some precedents

Using local PCA within a spectral clustering algorithm was implemented in four other publications we know of (Goldberg et al., 2009; Gong et al., 2012; Kushnir et al., 2006; Wang et al., 2011). As a first stage in their semi-supervised learning method, Goldberg, Zhu, Singh, Xu, and Nowak (2009) design a spectral clustering algorithm. The method starts by subsampling the data points, obtaining ‘centers’ in the following way. Draw \mathbf{y}_1 at random from the data and remove its ℓ -nearest neighbors from the data. Then repeat with the remaining data, obtaining centers $\mathbf{y}_1, \mathbf{y}_2, \dots$. Let \mathbf{C}_i denote the sample covariance in the neighborhood of \mathbf{y}_i made of its ℓ -nearest neighbors. An m -nearest-neighbor graph is then defined on the centers in terms of the Mahalanobis distances. Explicitly, the centers \mathbf{y}_i and \mathbf{y}_j are connected in the graph if \mathbf{y}_j is among the m nearest neighbors of \mathbf{y}_i in Mahalanobis distance

$$\|\mathbf{C}_i^{-1/2}(\mathbf{y}_i - \mathbf{y}_j)\|, \tag{1}$$

or vice-versa. The parameters ℓ and m are both chosen of order $\log n$. An existing edge between \mathbf{y}_i and \mathbf{y}_j is then weighted by $\exp(-H_{ij}^2/\eta^2)$, where H_{ij} denotes the Hellinger distance between the probability distributions $\mathcal{N}(\mathbf{0}, \mathbf{C}_i)$ and $\mathcal{N}(\mathbf{0}, \mathbf{C}_j)$. The spectral graph partitioning algorithm of Ng, Jordan, and Weiss (2002) — detailed in Algorithm 1 — is then applied to the resulting affinity matrix, with some form of constrained K-means. We note that Goldberg et al. (2009) evaluate their method in the context of semi-supervised learning where the clustering routine is only required to return subclusters of actual clusters. In particular, the data points other than the centers are discarded. Note also that their evaluation is empirical.

Algorithm 1 Spectral Graph Partitioning (Ng, Jordan, and Weiss, 2002)

Input:

Affinity matrix $\mathbf{W} = (W_{ij})$, size of the partition K

Steps:

- 1: Compute $\mathbf{Z} = (Z_{ij})$ according to $Z_{ij} = W_{ij}/\sqrt{D_i D_j}$, with $D_i = \sum_{j=1}^n W_{ij}$.
 - 2: Extract the top K eigenvectors of \mathbf{Z} .
 - 3: Renormalize each row of the resulting $n \times K$ matrix.
 - 4: Apply K -means to the row vectors.
-

The algorithm proposed by Kushnir, Galun, and Brandt (2006) is multiscale and works by coarsening the neighborhood graph and computing sampling density and geometric information inferred along the way such as obtained via PCA in local neighborhoods. This bottom-up flow is then followed by a top-down pass, and the two are iterated a few times. The algorithm is too complex to be described in detail here, and probably too complex to be analyzed mathematically.

The clustering methods of [Goldberg et al. \(2009\)](#) and ours can be seen as simpler variants that only go bottom up and coarsen the graph only once.

In the last stages of writing this paper, we learned of the works of [Wang, Jiang, Wu, and Zhou \(2011\)](#) and [Gong, Zhao, and Medioni \(2012\)](#), who propose algorithms very similar to our [Algorithm 3](#) detailed below. Note that these publications do not provide any theoretical guarantees for their methods, which is one of our main contributions here.

2.2 Our algorithms

We now describe our method and propose several variants. Our setting is standard: we observe data points $\mathbf{x}_1, \dots, \mathbf{x}_n \in \mathbb{R}^D$ that we assume were sampled in the vicinity of K smooth surfaces embedded in \mathbb{R}^D . The setting is formalized later in [Section 3.1](#).

2.2.1 Connected component extraction: comparing local covariances

We start with our simplest variant, which is also the most natural. The method depends on a neighborhood radius $r > 0$, a spatial scale parameter $\varepsilon > 0$ and a covariance (relative) scale $\eta > 0$. For a vector \mathbf{x} , $\|\mathbf{x}\|$ denotes its Euclidean norm, and for a (square) matrix \mathbf{A} , $\|\mathbf{A}\|$ denotes its spectral norm. For $n \in \mathbb{N}$, we denote by $[n]$ the set $\{1, \dots, n\}$. Given a data set $\mathbf{x}_1, \dots, \mathbf{x}_n$, for any point $\mathbf{x} \in \mathbb{R}^D$ and $r > 0$, define the neighborhood

$$N_r(\mathbf{x}) = \{\mathbf{x}_j : \|\mathbf{x} - \mathbf{x}_j\| \leq r\}. \tag{2}$$

Algorithm 2 Connected Component Extraction: Comparing Covariances

Input:

Data points $\mathbf{x}_1, \dots, \mathbf{x}_n$; neighborhood radius $r > 0$; spatial scale $\varepsilon > 0$, covariance scale $\eta > 0$.

Steps:

- 1: For each $i \in [n]$, compute the sample covariance matrix \mathbf{C}_i of $N_r(\mathbf{x}_i)$.
- 2: Compute the following affinities between data points:

$$W_{ij} = \mathbb{I}_{\{\|\mathbf{x}_i - \mathbf{x}_j\| \leq \varepsilon\}} \cdot \mathbb{I}_{\{\|\mathbf{C}_i - \mathbf{C}_j\| \leq \eta r^2\}}. \tag{3}$$

- 3: Remove \mathbf{x}_i when there is \mathbf{x}_j such that $\|\mathbf{x}_j - \mathbf{x}_i\| \leq r$ and $\|\mathbf{C}_j - \mathbf{C}_i\| > \eta r^2$.
 - 4: Extract the connected components of the resulting graph.
 - 5: Points removed in Step 3 are grouped with the closest point that survived Step 3.
-

In summary, the algorithm first creates an unweighted graph: the nodes of this graph are the data points and edges are formed between two nodes if both the distance between these nodes and the distance between the local covariance structures at these nodes are sufficiently small. After removing the points near the intersection at Step 3, the algorithm then extracts the connected components of the graph.

In principle, the neighborhood size r is chosen just large enough that performing PCA in each neighborhood yields a reliable estimate of the local covariance structure. For this, the number of points inside the neighborhood needs to be large enough, which depends on the sample size n , the sampling density, intrinsic dimension of the surfaces and their surface area (Hausdorff measure), how far the points are from the surfaces (i.e., noise level), and the regularity of the surfaces. The spatial scale parameter ε depends on the sampling density and r . It needs to be large enough that a

point has plenty of points within distance ε , including some across an intersection, so each cluster is strongly connected. At the same time, ε needs to be small enough that a local linear approximation to the surfaces is a relevant feature of proximity. Its choice is rather similar to the choice of the scale parameter in standard spectral clustering (Ng et al., 2002; Zelnik-Manor and Perona, 2004). The orientation scale η needs to be large enough that centers from the same cluster and within distance ε of each other have local covariance matrices within distance ηr^2 , but small enough that points from different clusters near their intersection have local covariance matrices separated by a distance substantially larger than ηr^2 . This depends on the curvature of the surfaces and the incidence angle at the intersection of two (or more) surfaces. Note that a typical covariance matrix over a ball of radius r has norm of order r^2 , which justifies using our choice of parametrization. In the mathematical framework we introduce later on, these parameters can be chosen automatically as done in (Arias-Castro et al., 2011), at least when the points are sampled exactly on the surfaces. We will not elaborate on that since in practice this does not inform our choice of parameters.

The rationale behind Step 3 is as follows. As we just discussed, the parameters need to be tuned so that points from the same cluster and within distance ε have local covariance matrices within distance ηr^2 . Hence, \mathbf{x}_i and \mathbf{x}_j in Step 3 are necessarily from different clusters. Since they are near each other, in our model this will imply that they are close to an intersection. Therefore, roughly speaking, Step 3 removes points near an intersection.

Although this method works in simple situations like that of two intersecting segments (Figure 1), it is not meant to be practical. Indeed, extracting connected components is known to be sensitive to spurious points and therefore unstable. Furthermore, we found that comparing local covariance matrices as in affinity (3) tends to be less stable than comparing local projections as in affinity (4), which brings us to our next variant.

2.2.2 Connected component extraction: comparing local projections

We present another variant also based on extracting the connected components of a neighborhood graph that compares orthogonal projections onto the largest principal directions.

Algorithm 3 Connected Component Extraction: Comparing Projections

Input:

Data points $\mathbf{x}_1, \dots, \mathbf{x}_n$; neighborhood radius $r > 0$, spatial scale $\varepsilon > 0$, projection scale $\eta > 0$.

Steps:

- 1: For each $i \in [n]$, compute the sample covariance matrix \mathbf{C}_i of $N_r(\mathbf{x}_i)$.
- 2: Compute the projection \mathbf{Q}_i onto the eigenvectors of \mathbf{C}_i with eigenvalue exceeding $\sqrt{\eta} \|\mathbf{C}_i\|$.
- 3: Compute the following affinities between data points:

$$W_{ij} = \mathbb{I}_{\{\|\mathbf{x}_i - \mathbf{x}_j\| \leq \varepsilon\}} \cdot \mathbb{I}_{\{\|\mathbf{Q}_i - \mathbf{Q}_j\| \leq \eta\}}. \quad (4)$$

- 4: Extract the connected components of the resulting graph.
-

We note that the local intrinsic dimension is determined by thresholding the eigenvalues of the local covariance matrix, keeping the directions with eigenvalues within some range of the largest eigenvalue. The same strategy is used by Kushnir et al. (2006), but with a different threshold. The method is a hard version of what we implemented, which we describe next.

2.2.3 Covariances or projections?

In our numerical experiments, we tried working both directly with covariance matrices as in (3) and with projections as in (4). Note that in our experiments we used spectral graph partitioning with soft versions of these affinities, as described in Section 2.2.4. We found working with projections to be more reliable. The problem comes, in part, from boundaries. When a surface has a boundary, local covariances over neighborhoods that overlap with the boundary are quite different from local covariances over nearby neighborhoods that do not touch the boundary. Consider the example of two segments, S_1 and S_2 , intersecting at an angle of $\theta \in (0, \pi/2)$ at their middle point, specifically

$$S_1 = [-1, 1] \times \{0\}, \quad S_2 = \{(x, x \tan \theta) : x \in [-\cos \theta, \cos \theta]\}.$$

Assume there is no noise and that the sampling is uniform. Assume $r \in (0, \frac{1}{2} \sin \theta)$ so that the disc centered at $\mathbf{x}_1 := (1/2, 0)$ does not intersect S_2 , and the disc centered at $\mathbf{x}_2 := (\frac{1}{2} \cos \theta, \frac{1}{2} \tan \theta)$ does not intersect S_1 . Let $\mathbf{x}_0 = (1, 0)$. For $\mathbf{x} \in S_1 \cup S_2$, let $\mathbf{C}_{\mathbf{x}}$ denote the local covariance at \mathbf{x} over a ball of radius r . Simple calculations yield:

$$\mathbf{C}_{(1,0)} = \frac{r^2}{12} \begin{pmatrix} 1 & 0 \\ 0 & 0 \end{pmatrix}, \quad \mathbf{C}_{\mathbf{x}_1} = \frac{r^2}{3} \begin{pmatrix} 1 & 0 \\ 0 & 0 \end{pmatrix}, \quad \mathbf{C}_{\mathbf{x}_2} = \frac{r^2}{3} \begin{pmatrix} \cos^2 \theta & \sin(\theta) \cos(\theta) \\ \sin(\theta) \cos(\theta) & \sin^2 \theta \end{pmatrix},$$

and therefore

$$\|\mathbf{C}_{\mathbf{x}_0} - \mathbf{C}_{\mathbf{x}_1}\| = \frac{r^2}{4}, \quad \|\mathbf{C}_{\mathbf{x}_1} - \mathbf{C}_{\mathbf{x}_2}\| = \frac{\sqrt{2}r^2}{3} \sin \theta.$$

When $\sin \theta \leq \frac{3}{4\sqrt{2}}$ (roughly, $\theta \leq 32^\circ$), the difference in Frobenius norm between the local covariances at $\mathbf{x}_0, \mathbf{x}_1 \in S_1$ is larger than that at $\mathbf{x}_1 \in S_1$ and $\mathbf{x}_2 \in S_2$. As for projections, however,

$$\mathbf{Q}_{\mathbf{x}_0} = \mathbf{Q}_{\mathbf{x}_1} = \begin{pmatrix} 1 & 0 \\ 0 & 0 \end{pmatrix}, \quad \mathbf{Q}_{\mathbf{x}_2} = \begin{pmatrix} \cos^2 \theta & \sin(\theta) \cos(\theta) \\ \sin(\theta) \cos(\theta) & \sin^2 \theta \end{pmatrix},$$

so that

$$\|\mathbf{Q}_{\mathbf{x}_0} - \mathbf{Q}_{\mathbf{x}_1}\| = 0, \quad \|\mathbf{Q}_{\mathbf{x}_1} - \mathbf{Q}_{\mathbf{x}_2}\| = \sqrt{2} \sin \theta.$$

While in theory the boundary points account for a small portion of the sample, in practice this is not the case and we find that spectral graph partitioning is challenged by having points near the boundary that are far (in affinity) from nearby points from the same cluster. This may explain why the (soft version of) affinity (4) yields better results than the (soft version of) affinity (3) in our experiments.

2.2.4 Spectral Clustering Based on Local PCA

The following variant is more robust in practice and is the algorithm we actually implemented. The method assumes that the surfaces are of same dimension d and that they are K surfaces, with both parameters K and d known.

We note that $\mathbf{y}_1, \dots, \mathbf{y}_{n_0}$ forms an r -packing of the data. The underlying rationale for this coarsening is justified in (Goldberg et al., 2009) by the fact that the covariance matrices, and also the top principal directions, change smoothly with the location of the neighborhood, so that without subsampling these characteristics would not help detect the abrupt event of an intersection. The affinity (5) is of course a soft version of (4).

Algorithm 4 Spectral Clustering Based on Local PCA

Input:

Data points $\mathbf{x}_1, \dots, \mathbf{x}_n$; neighborhood radius $r > 0$; spatial scale $\varepsilon > 0$, projection scale $\eta > 0$; intrinsic dimension d ; number of clusters K .

Steps:

0: Pick one point \mathbf{y}_1 at random from the data. Pick another point \mathbf{y}_2 among the data points not included in $N_r(\mathbf{y}_1)$, and repeat the process, selecting centers $\mathbf{y}_1, \dots, \mathbf{y}_{n_0}$.

1: For each $i = 1, \dots, n_0$, compute the sample covariance matrix \mathbf{C}_i of $N_r(\mathbf{y}_i)$. Let \mathbf{Q}_i denote the orthogonal projection onto the space spanned by the top d eigenvectors of \mathbf{C}_i .

2: Compute the following affinities between center pairs:

$$W_{ij} = \exp\left(-\frac{\|\mathbf{y}_i - \mathbf{y}_j\|^2}{\varepsilon^2}\right) \cdot \exp\left(-\frac{\|\mathbf{Q}_i - \mathbf{Q}_j\|^2}{\eta^2}\right). \quad (5)$$

3: Apply spectral graph partitioning (Algorithm 1) to \mathbf{W} .

4: The data points are clustered according to the closest center in Euclidean distance.

2.2.5 Comparison with closely related methods

We highlight some differences with the other proposals in the literature. We first compare our approach to that of Goldberg et al. (2009), which was our main inspiration.

- *Neighborhoods.* Comparing with Goldberg et al. (2009), we define neighborhoods over r -balls instead of ℓ -nearest neighbors, and connect points over ε -balls instead of m -nearest neighbors. This choice is for convenience, as these ways are in fact essentially equivalent when the sampling density is fairly uniform. This is elaborated at length in (Arias-Castro, 2011; Brito et al., 1997; Maier et al., 2009).
- *Mahalanobis distances.* Goldberg et al. (2009) use Mahalanobis distances (1) between centers. In our version, we could for example replace the Euclidean distance $\|\mathbf{x}_i - \mathbf{x}_j\|$ in the affinity (3) with the average Mahalanobis distance

$$\|\mathbf{C}_i^{-1/2}(\mathbf{x}_i - \mathbf{x}_j)\| + \|\mathbf{C}_j^{-1/2}(\mathbf{x}_j - \mathbf{x}_i)\|. \quad (6)$$

We actually tried this and found that the algorithm was less stable, particularly under low noise. Introducing a regularization in this distance — which requires the introduction of another parameter — solves this problem partially.

That said, using Mahalanobis distances makes the procedure less sensitive to the choice of ε , in that neighborhoods may include points from different clusters. Think of two parallel line segments separated by a distance of δ , and assume there is no noise, so the points are sampled exactly from these segments. Assuming an infinite sample size, the local covariance is the same everywhere so that points within distance ε are connected by the affinity (3). Hence, Algorithm 2 requires that $\varepsilon < \delta$. In terms of Mahalanobis distances, points on different segments are infinitely separated, so a version based on these distances would work with any $\varepsilon > 0$. In the case of curved surfaces and/or noise, the situation is similar, though not as evident. Even then, the gain in performance guarantees is not obvious, since we only require that ε be slightly larger in order of magnitude than r .

- *Hellinger distances.* As we mentioned earlier, [Goldberg et al. \(2009\)](#) use Hellinger distances of the probability distributions $\mathcal{N}(\mathbf{0}, \mathbf{C}_i)$ and $\mathcal{N}(\mathbf{0}, \mathbf{C}_j)$ to compare covariance matrices, specifically

$$\left(1 - 2^{D/2} \frac{\det(\mathbf{C}_i \mathbf{C}_j)^{1/4}}{\det(\mathbf{C}_i + \mathbf{C}_j)^{1/2}}\right)^{1/2}, \quad (7)$$

if \mathbf{C}_i and \mathbf{C}_j are full-rank. While using these distances or the Frobenius distances makes little difference in practice, we find it easier to work with the latter when it comes to proving theoretical guarantees. Moreover, it seems more natural to assume a uniform sampling distribution in each neighborhood rather than a normal distribution, so that using the more sophisticated similarity (7) does not seem justified.

- *K-means.* We use K-means++ for a good initialization. However, we found that the more sophisticated size-constrained K-means ([Bradley et al., 2000](#)) used in ([Goldberg et al., 2009](#)) did not improve the clustering results.

As we mentioned above, our work was developed in parallel to that of [Wang et al. \(2011\)](#) and [Gong et al. \(2012\)](#). We highlight some differences. They do not subsample, but estimate the local tangent space at each data point \mathbf{x}_i . [Wang et al. \(2011\)](#) fit a mixture of d -dimensional affine subspaces to the data using MPPCA ([Tipping and Bishop, 1999](#)), which is then used to estimate the tangent subspaces at each data point. [Gong et al. \(2012\)](#) develop some sort of robust local PCA. While [Wang et al. \(2011\)](#) assume all surfaces are of same dimension known to the user, [Gong et al. \(2012\)](#) estimate that locally by looking at the largest gap in the spectrum of estimated local covariance matrix. This is similar in spirit to what is done in Step 2 of Algorithm 3, but we did not include this step in Algorithm 4 because we did not find it reliable in practice. We also tried estimating the local dimensionality using the method of [Little et al. \(2009\)](#), but this failed in the most complex cases.

[Wang et al. \(2011\)](#) use a nearest-neighbor graph and their affinity is defined as

$$W_{ij} = \Delta_{ij} \cdot \left(\prod_{s=1}^d \cos \theta_s(i, j)\right)^\alpha, \quad (8)$$

where $\Delta_{ij} = 1$ if \mathbf{x}_i is among the ℓ -nearest neighbors of \mathbf{x}_j , or vice versa, while $\Delta_{ij} = 0$ otherwise; $\theta_1(i, j) \geq \dots \geq \theta_d(i, j)$ are the principal (aka, canonical) angles ([Stewart and Sun, 1990](#)) between the estimated tangent subspaces at \mathbf{x}_i and \mathbf{x}_j . ℓ and α are parameters of the method. [Gong et al. \(2012\)](#) define an affinity that incorporates the self-tuning method of [Zelnik-Manor and Perona \(2004\)](#); in our notation, their affinity is

$$\exp\left(-\frac{\|\mathbf{x}_i - \mathbf{x}_j\|^2}{\varepsilon_i \varepsilon_j}\right) \cdot \exp\left(-\frac{\text{asin}^2 \|\mathbf{Q}_i - \mathbf{Q}_j\|}{\eta^2 \|\mathbf{x}_i - \mathbf{x}_j\|^2 / (\varepsilon_i \varepsilon_j)}\right). \quad (9)$$

where ε_i is the distance from \mathbf{x}_i to its ℓ -nearest neighbor. ℓ is a parameter.

Although we do not analyze their respective ways of estimating the tangent subspaces, our analysis provides essential insights into their methods, and for that matter, any other method built on spectral clustering based on tangent subspace comparisons.

3 Mathematical Analysis

While the analysis of Algorithm 4 seems within reach, there are some complications due to the fact that points near the intersection may form a cluster of their own — we were not able to discard this

possibility. Instead, we study the simpler variants described in Algorithm 2 and Algorithm 3. Even then, the arguments are rather complex and interestingly involved. The theoretical guarantees that we thus obtain for these variants are stated in Theorem 1 and proved in Section 6. We comment on the analysis of Algorithm 4 right after that. We note that there are very few theoretical results on resolving intersecting clusters. In fact, we are only aware of (Chen and Lerman, 2009a) in the context of affine surfaces, (Soltanolkotabi and Candès, 2011) in the context of affine surfaces without noise and (Arias-Castro et al., 2011) in the context of curves.

The generative model we assume is a natural mathematical framework for multi-manifold learning where points are sampled in the vicinity of smooth surfaces embedded in Euclidean space. For concreteness and ease of exposition, we focus on the situation where two surfaces (i.e., $K = 2$) of same dimension $1 \leq d \leq D$ intersect. This special situation already contains all the geometric intricacies of separating intersecting clusters. On the one hand, clusters of different intrinsic dimension may be separated with an accurate estimation of the local intrinsic dimension without further geometry involved (Haro et al., 2007). On the other hand, more complex intersections (3-way and higher) complicate the situation without offering truly new challenges. For simplicity of exposition, we assume that the surfaces are submanifolds without boundary, though it will be clear from the analysis (and the experiments) that the method can handle surfaces with (smooth) boundaries that may self-intersect. We discuss other possible extensions in Section 5.

Within that framework, we show that Algorithm 2 and Algorithm 3 are able to identify the clusters accurately except for points near the intersection. Specifically, with high probability with respect to the sampling distribution, Algorithm 2 divides the data points into two groups such that, except for points within distance $C\varepsilon$ of the intersection, all points from the first cluster are in one group and all points from the second cluster are in the other group. The constant C depends on the surfaces, including their curvatures, separation between them and intersection angle. The situation for Algorithm 3 is more complex, as it may return more than two clusters, but the main feature is that most of two clusters (again, away from the intersection) are in separate connected components.

3.1 Generative model

Each surface we consider is a connected, C^2 and compact submanifold without boundary and of dimension d embedded in \mathbb{R}^D . Any such surface has a positive reach, which is what we use to quantify smoothness. The notion of reach was introduced by Federer (1959). Intuitively, a surface has reach exceeding r if, and only if, one can roll a ball of radius r on the surface without obstruction (Walther, 1997). Formally, for $\mathbf{x} \in \mathbb{R}^D$ and $S \subset \mathbb{R}^D$, let

$$\text{dist}(\mathbf{x}, S) = \inf_{\mathbf{s} \in S} \|\mathbf{x} - \mathbf{s}\|,$$

and

$$B(S, r) = \{\mathbf{x} : \text{dist}(\mathbf{x}, S) < r\},$$

which is often called the r -tubular neighborhood (or r -neighborhood) of S . The reach of S is the supremum over $r > 0$ such that, for each $\mathbf{x} \in B(S, r)$, there is a unique point in S nearest \mathbf{x} . It is well-known that, for C^2 submanifolds, the reach bounds the radius of curvature from below (Federer, 1959, Lem. 4.17). For submanifolds without boundaries, the reach coincides with the condition number introduced in (Niyogi et al., 2008).

When two surfaces S_1 and S_2 intersect, meaning $S_1 \cap S_2 \neq \emptyset$, we define their incidence angle as

$$\theta(S_1, S_2) := \inf (\theta_{\min}(T_{S_1}(\mathbf{s}), T_{S_2}(\mathbf{s})) : \mathbf{s} \in S_1 \cap S_2), \quad (10)$$

where $T_S(\mathbf{s})$ denote the tangent subspace of submanifold S at point $\mathbf{s} \in S$, and $\theta_{\min}(T_1, T_2)$ is the smallest *nonzero* principal (aka, canonical) angle between subspaces T_1 and T_2 (Stewart and Sun, 1990).

The clusters are generated as follows. Each data point \mathbf{x}_i is drawn according to

$$\mathbf{x}_i = \mathbf{s}_i + \mathbf{z}_i, \tag{11}$$

where \mathbf{s}_i is drawn from the uniform distribution over $S_1 \cup S_2$ and \mathbf{z}_i is an additive noise term satisfying $\|\mathbf{z}_i\| \leq \tau$ — thus τ represents the noise or jitter level, and $\tau = 0$ means that the points are sampled on the surfaces. We assume the points are sampled independently of each other. We let

$$I_k = \{i : \mathbf{s}_i \in S_k\}, \tag{12}$$

and the goal is to recover the groups I_1 and I_2 , up to some errors.

3.2 Performance guarantees

We state some performance guarantees for Algorithm 2 and Algorithm 3.

Theorem 1. *Consider two connected, compact, twice continuously differentiable submanifolds without boundary, of same dimension, intersecting at a strictly positive angle, with the intersection set having strictly positive reach. Assume the parameters are set so that*

$$\tau \leq r\eta/C, \quad r \leq \varepsilon/C, \quad \varepsilon \leq \eta/C, \quad \eta \leq 1/C, \tag{13}$$

and $C > 0$ is large enough. Then with probability at least $1 - Cn \exp[-nr^d\eta^2/C]$:

- Algorithm 2 returns exactly two groups such that two points from different clusters are not grouped together unless one of them is within distance Cr from the intersection.
- Algorithm 3 returns at least two groups, and such that two points from different clusters are not grouped together unless one of them is within distance Cr from the intersection.

We note that the constant $C > 0$ depends on what configuration the surfaces are in, in particular their reach and intersection angle, but also aspects that are harder to quantify, like their separation away from their intersection.

We now comment on the challenge of proving a similar result for Algorithm 4. This algorithm relies on knowledge of the intrinsic dimension of the surfaces d and the number of clusters (here $K = 2$), but these may be estimated as in (Arias-Castro et al., 2011), at least in theory, so we assume these parameters are known. The subsampling done in Step 0 does not pose any problem whatsoever, since the centers are well-spread when the points themselves are. The difficulty resides in the application of the spectral graph partitioning, Algorithm 1. If we were to include the intersection-removal step (Step 3 of Algorithm 2) before applying spectral graph partitioning, then a simple adaptation of arguments in (Arias-Castro, 2011) would suffice. The real difficulty, and potential pitfall of the method in this framework (without the intersection-removal step), is that the points near the intersection may form their own cluster. For example, in the simplest case of two affine surfaces intersecting at a positive angle and no sampling noise, the projection matrix at a point near the intersection — meaning a point whose r -ball contains a substantial piece of both surfaces — would be the projection matrix onto $S_1 + S_2$ seen as a linear subspace. We were not able to discard this possibility, although we do not observe this happening in practice. A possible remedy is to constrain the K-means part to only return large-enough clusters. However, a proper analysis of this would require a substantial amount of additional work and we did not engage seriously in this pursuit.

4 Numerical Experiments

We tried our code[§] on a few artificial examples. Very few algorithms were designed to work in the general situation we consider here and we did not compare our method with any other. As we argued earlier, the methods of Wang et al. (2011) and Gong et al. (2012) are quite similar to ours, and we encourage the reader to also look at the numerical experiments they performed. Our numerical experiments should be regarded as a proof of concept, only here to show that our method can be implemented and works on some toy examples.

In all experiments, the number of clusters K and the dimension of the manifolds d are assumed known. We choose spatial scale ε and the projection scale η automatically as follows: we let

$$\varepsilon = \max_{1 \leq i \leq n_0} \min_{j \neq i} \|\mathbf{y}_i - \mathbf{y}_j\|, \quad (14)$$

and

$$\eta = \operatorname{median}_{(i,j): \|\mathbf{y}_i - \mathbf{y}_j\| < \varepsilon} \|\mathbf{P}_i - \mathbf{P}_j\|. \quad (15)$$

Here, we implicitly assume that the union of all the underlying surfaces forms a connected set. In that case, the idea behind choosing ε as in (14) is that we want the ε -graph on the centers $\mathbf{y}_1, \dots, \mathbf{y}_n$ to be connected. Then η is chosen so that a center \mathbf{y}_i remains connected in the (ε, η) -graph to most of its neighbors in the ε -graph.

The neighborhood radius r is chosen by hand for each situation. Although we do not know how to choose r automatically, there are some general ad hoc guidelines. When r is too large, the local linear approximation to the underlying surfaces may not hold in neighborhoods of radius r , resulting in local PCA becoming inappropriate. When r is too small, there might not be enough points in a neighborhood of radius r to accurately estimate the local tangent subspace to a given surface at that location, resulting in local PCA becoming inaccurate. From a computational point of view, the smaller r , the larger the number of neighborhoods and the heavier the computations, particularly at the level of spectral graph partitioning. In our numerical experiments, we find that our algorithm is more sensitive to the choice of r when the clustering problem is more difficult. We note that automatic choice of tuning parameters remains a challenge in clustering, and machine learning at large, especially when no labels are available whatsoever. See (Kaslovsky and Meyer, 2011; Little et al., 2009; Zelnik-Manor and Perona, 2004; Zhang et al., 2012).

Since the algorithm is randomized (see Step 0 in Algorithm 4) we repeat each simulation 100 times and report the median misclustering rate and number of times where the misclustering rate is smaller than 5%, 10%, and 15%.

We first run Algorithm 4 on several artificial data sets, which are demonstrated in the LHS of Figures 2 and 3. Table 1 reports the local radius r used for each data set (R is the global radius of each data set), and the statistics for misclustering rates. Typical clustering results are demonstrated in the RHS of Figures 2 and 3. It is evident that Algorithm 4 performs well in these simulations.

In another simulation, we show the dependence of the success of our algorithm on the intersecting angle between curves in Table 2 and Figure 4. Here, we fix two curves intersecting at a point, and gradually decrease the intersection angle by rotating one of them while holding the other one fixed. The angles are $\pi/2$, $\pi/4$, $\pi/6$ and $\pi/8$. From the table we can see that our algorithm performs well when the angle is $\pi/4$, but the performance deteriorates as the angle becomes smaller, and the algorithm almost always fails when the angle is $\pi/8$.

[§]The code is available online at <http://www.ima.umn.edu/~zhang620/>.

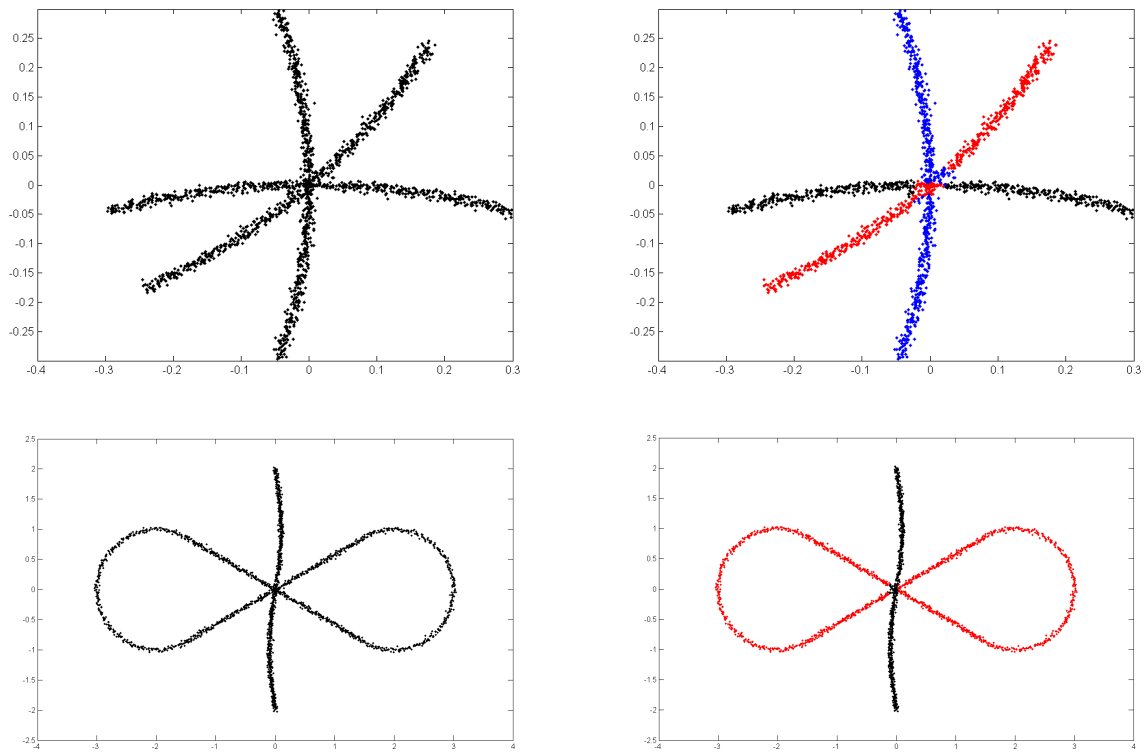


Figure 2: Performance of Algorithm 4 on data sets “Three curves” and “Self-intersecting curves”. Left column is the input data sets, and right column demonstrates the typical clustering.

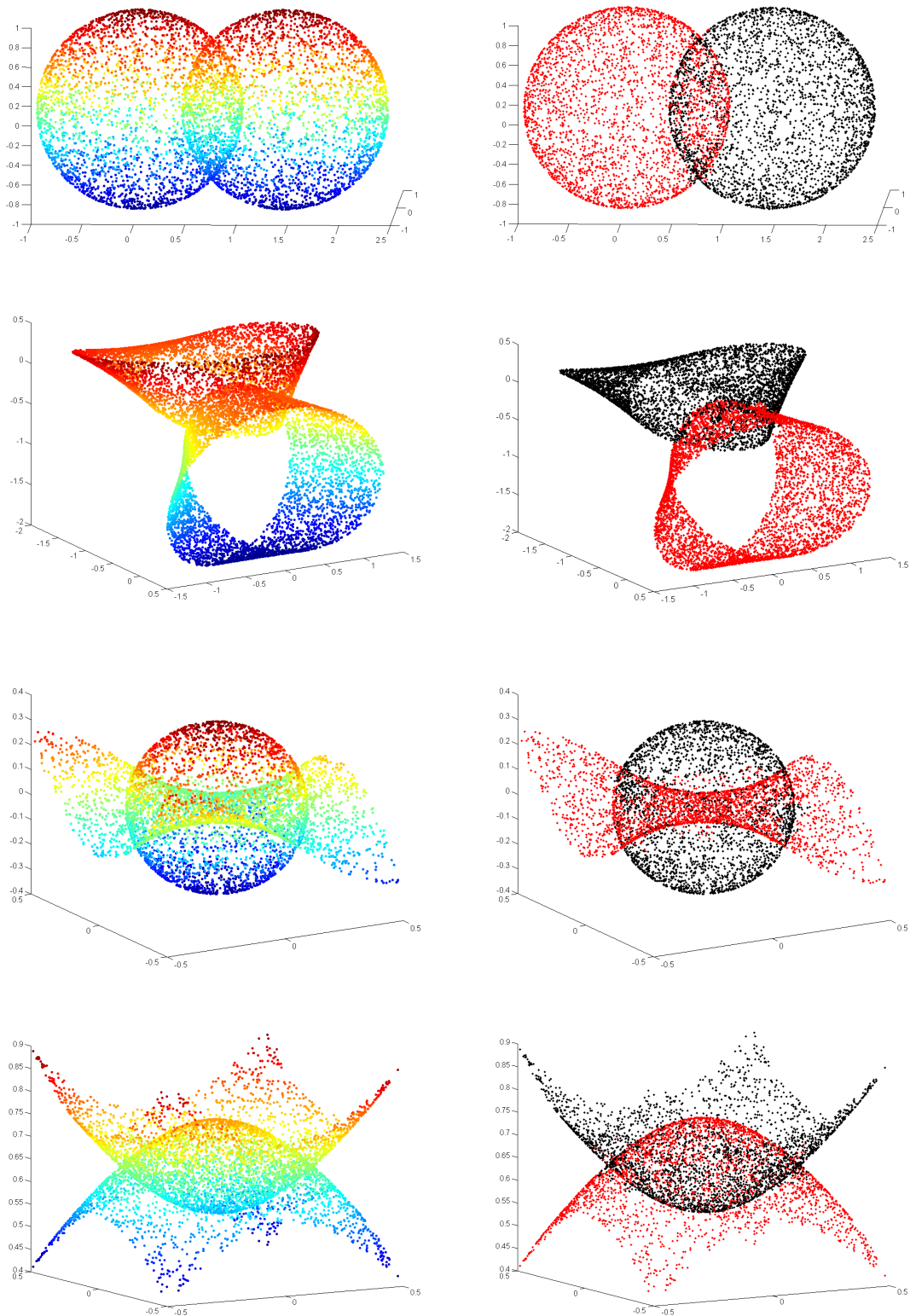


Figure 3: Performance of Algorithm 4 on data sets “Two spheres”, “Mobius strips”, “Monkey saddle” and “Paraboloids”. Left column is the input data sets, and right column demonstrates the typical clustering.

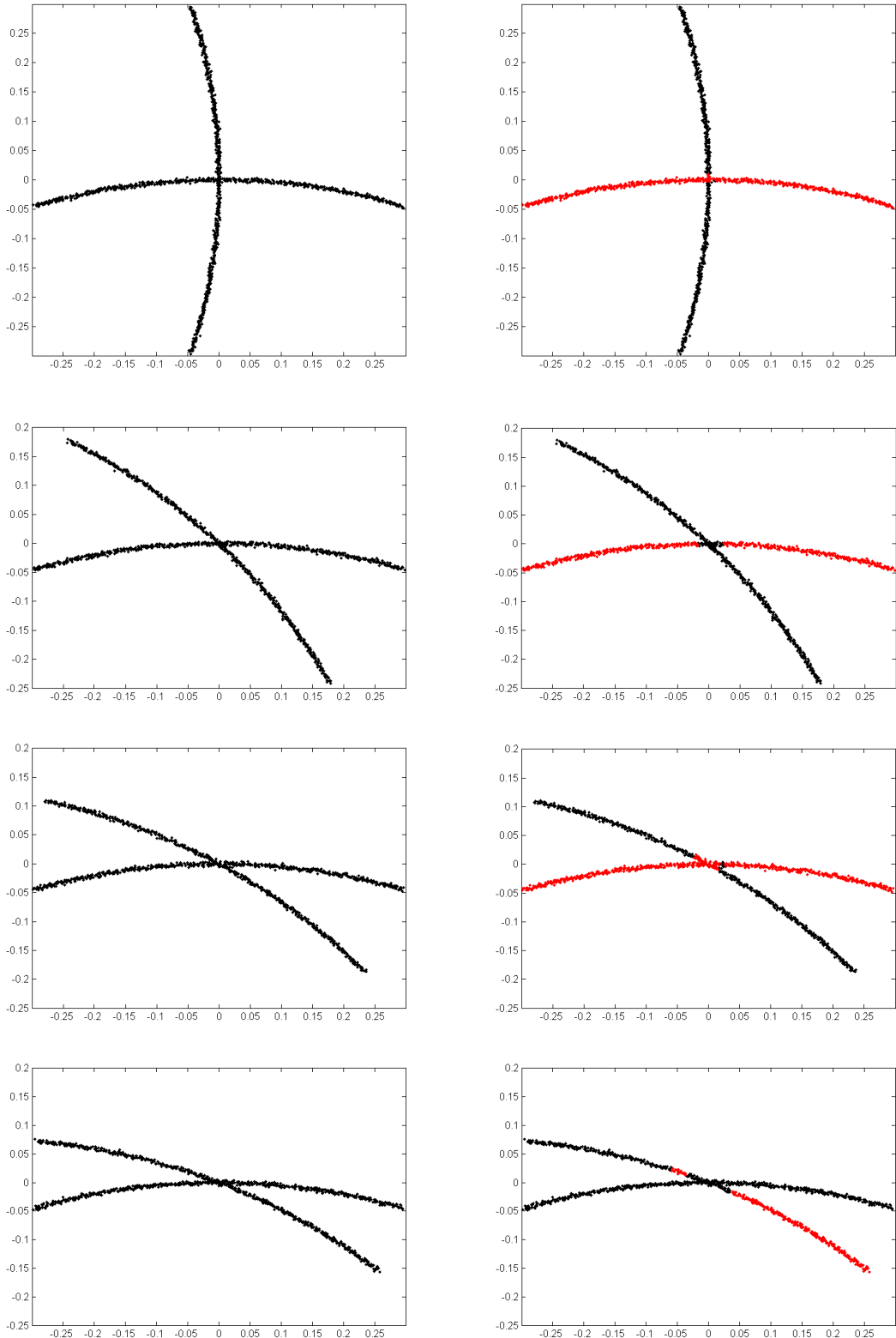


Figure 4: Performance of Algorithm 4 on two curves intersecting at various angles $\frac{\pi}{2}$, $\frac{\pi}{4}$, $\frac{\pi}{6}$, $\frac{\pi}{8}$.

dataset	r	median misclustering rate	5%	10%	15%
Three curves	0.02 (0.034 <i>R</i>)	4.16%	76	89	89
Self-intersecting curves	0.1 (0.017 <i>R</i>)	1.16%	85	85	86
Two spheres	0.2 (0.059 <i>R</i>)	3.98%	100	100	100
Mobius strips	0.1 (0.028 <i>R</i>)	2.22%	85	86	88
Monkey saddle	0.1 (0.069 <i>R</i>)	9.73%	0	67	97
Paraboloids	0.07 (0.048 <i>R</i>)	10.42%	0	12	91

Table 1: Choices for r and misclustering statistics for the artificial data sets demonstrated in Figures 2 and 3. The statistics are based on 100 repeats and include the median misclustering rate and number of repeats where the misclustering rate is smaller than 5%, 10% and 15%.

Intersecting angle	r	median misclustering rate	5%	10%	15%
$\pi/2$	0.02 (0.034 <i>R</i>)	2.08%	98	98	98
$\pi/4$	0.02 (0.034 <i>R</i>)	3.33%	92	94	94
$\pi/6$	0.02 (0.034 <i>R</i>)	5.53%	32	59	59
$\pi/8$	0.02 (0.033 <i>R</i>)	27.87%	0	2	2

Table 2: Choices for r and misclustering statistics for the instances of two intersecting curves demonstrated in Figure 4. The statistics are based on 100 repeats and include the median misclustering rate and number of repeats where the misclustering rate is smaller than 5%, 10% and 15%.

5 Discussion

We distilled the ideas of Goldberg et al. (2009) and of Kushnir et al. (2006) to cluster points sampled near smooth surfaces. The key ingredient is the use of local PCA to learn about the local spread and orientation of the data, so as to use that information in an affinity when building a neighborhood graph.

In a typical stylized setting for multi-manifold clustering, we established performance bounds for the simple variants described in Algorithm 2 and Algorithm 3, which essentially consist of connecting points that are close in space and orientation, and then extracting the connected components of the resulting graph. Both are shown to resolve general intersections as long as the incidence angle is strictly positive and the parameters are carefully chosen. As is commonly the case in such analyzes, our setting can be generalized to other sampling schemes, to multiple intersections, to some features of the surfaces changing with the sample size, and so on, in the spirit of (Arias-Castro, 2011; Arias-Castro et al., 2011; Chen and Lerman, 2009a). We chose to simplify the setup as much as possible while retaining the essential features that makes resolving intersecting clusters challenging. The resulting arguments are nevertheless rich enough to satisfy the mathematically thirsty reader.

We implemented a spectral version of Algorithm 3, described in Algorithm 4, that assumes the intrinsic dimensionality and the number of clusters are known. The resulting approach is very similar to what is offered by Wang et al. (2011) and Gong et al. (2012), although it was developed independently of these works. Algorithm 4 is shown to perform well in some simulated experiments, although it is somewhat sensitive to the choice of parameters. This is the case of all other methods for multi-manifold clustering we know of and choosing the parameters automatically remains an open challenge in the field.

6 Proofs

We start with some additional notation. The ambient space is \mathbb{R}^D unless noted otherwise. For a vector $\mathbf{v} \in \mathbb{R}^D$, $\|\mathbf{v}\|$ denotes its Euclidean norm and for a real matrix $\mathbf{M} \in \mathbb{R}^{D \times D}$, $\|\mathbf{M}\|$ denotes the corresponding operator norm. For a point $\mathbf{x} \in \mathbb{R}^D$ and $r > 0$, $B(\mathbf{x}, r)$ denotes the open ball of center \mathbf{x} and radius r , i.e., $B(\mathbf{x}, r) = \{\mathbf{y} \in \mathbb{R}^D : \|\mathbf{y} - \mathbf{x}\| < r\}$. For a set S and a point \mathbf{x} , define $\text{dist}(\mathbf{x}, S) = \inf\{\|\mathbf{x} - \mathbf{y}\| : \mathbf{y} \in S\}$. For two points \mathbf{a}, \mathbf{b} in the same Euclidean space, $\mathbf{b} - \mathbf{a}$ denotes the vector moving \mathbf{a} to \mathbf{b} . For a point \mathbf{a} and a vector \mathbf{v} in the same Euclidean space, $\mathbf{a} + \mathbf{v}$ denotes the translate of \mathbf{a} by \mathbf{v} . We identify an affine subspace T with its corresponding linear subspace, for example, when saying that a vector belongs to T .

For two subspaces T and T' , of possibly different dimensions, we denote by $0 \leq \theta_{\max}(T, T') \leq \pi/2$ the largest and by $\theta_{\min}(T, T')$ the smallest nonzero principal angle between T and T' (Stewart and Sun, 1990). When \mathbf{v} is a vector and T is a subspace, $\angle(\mathbf{v}, T) := \theta_{\max}(\mathbb{R}\mathbf{v}, T)$ this is the usual definition of the angle between \mathbf{v} and T .

For a subset $A \subset \mathbb{R}^D$ and positive integer d , $\text{vol}_d(A)$ denotes the d -dimensional Hausdorff measure of A , and $\text{vol}(A)$ is defined as $\text{vol}_{\dim(A)}(A)$, where $\dim(A)$ is the Hausdorff dimension of A . For a Borel set A , let λ_A denote the uniform distribution on A .

For a set $S \subset \mathbb{R}^D$ with reach at least $1/\kappa$, and \mathbf{x} with $\text{dist}(\mathbf{x}, S) < 1/\kappa$, let $P_S(\mathbf{x})$ denote the metric projection of \mathbf{x} onto S , that is, the point on S closest to \mathbf{x} . Note that, if T is an affine subspace, then P_T is the usual orthogonal projection onto T . Let $\mathcal{S}_d(\kappa)$ denote the class of connected, C^2 and compact d -dimensional submanifolds without boundary embedded in \mathbb{R}^D , with reach at least $1/\kappa$. For a submanifold $S \in \mathcal{S}_d(\kappa)$, let $T_S(\mathbf{x})$ denote the tangent space of S at $\mathbf{x} \in S$.

We will often identify a linear map with its matrix in the canonical basis. For a symmetric (real) matrix \mathbf{M} , let $\beta_1(\mathbf{M}) \geq \beta_2(\mathbf{M}) \geq \dots$ denote its eigenvalues in decreasing order.

We say that $f : \Omega \subset \mathbb{R}^D \rightarrow \mathbb{R}^D$ is C -Lipschitz if $\|f(\mathbf{x}) - f(\mathbf{y})\| \leq C\|\mathbf{x} - \mathbf{y}\|, \forall \mathbf{x}, \mathbf{y} \in \Omega$.

For two reals a and b , $a \vee b = \max(a, b)$ and $a \wedge b = \min(a, b)$. Additional notation will be introduced as needed.

6.1 Preliminaries

This section gathers a number of general results from geometry and probability. We took time to package them into standalone lemmas that could be of potential independent interest, particularly to researchers working in machine learning and computational geometry.

6.1.1 Smooth surfaces and their tangent subspaces

The following result is on approximating a smooth surface near a point by the tangent subspace at that point. It is based on (Federer, 1959, Th. 4.18(2)).

Lemma 1. *For $S \in \mathcal{S}_d(\kappa)$, and any two points $\mathbf{s}, \mathbf{s}' \in S$,*

$$\text{dist}(\mathbf{s}', T_S(\mathbf{s})) \leq \frac{\kappa}{2} \|\mathbf{s}' - \mathbf{s}\|^2, \quad (16)$$

and when $\text{dist}(\mathbf{s}', T_S(\mathbf{s})) \leq 1/\kappa$,

$$\text{dist}(\mathbf{s}', T_S(\mathbf{s})) \leq \kappa \|P_{T_S(\mathbf{s})}(\mathbf{s}') - \mathbf{s}\|^2. \quad (17)$$

Moreover, for $\mathbf{t} \in T_S(\mathbf{s})$ such that $\|\mathbf{s} - \mathbf{t}\| \leq 7/(16\kappa)$,

$$\text{dist}(\mathbf{t}, S) \leq \kappa \|\mathbf{t} - \mathbf{s}\|^2. \quad (18)$$

Proof. Let T be short for $T_S(\mathbf{s})$. (Federer, 1959, Th. 4.18(2)) says that

$$\text{dist}(\mathbf{s}' - \mathbf{s}, T) \leq \frac{\kappa}{2} \|\mathbf{s}' - \mathbf{s}\|^2. \quad (19)$$

Immediately, we have

$$\text{dist}(\mathbf{s}' - \mathbf{s}, T) = \|\mathbf{s}' - P_T(\mathbf{s}')\| = \text{dist}(\mathbf{s}', T),$$

and (16) comes from that. Based on that and Pythagoras theorem, we have

$$\text{dist}(\mathbf{s}', T) = \|P_T(\mathbf{s}') - \mathbf{s}'\| \leq \frac{\kappa}{2} \|\mathbf{s}' - \mathbf{s}\|^2 = \frac{\kappa}{2} (\|P_T(\mathbf{s}') - \mathbf{s}'\|^2 + \|P_T(\mathbf{s}') - \mathbf{s}\|^2),$$

so that

$$\text{dist}(\mathbf{s}', T) \left(1 - \frac{\kappa}{2} \text{dist}(\mathbf{s}', T)\right) \leq \frac{\kappa}{2} \|P_T(\mathbf{s}') - \mathbf{s}\|^2,$$

and (17) follows easily from that. For (18), let $\mathbf{s}' = P_T^{-1}(\mathbf{t})$, which is well-defined by Lemma 3 below and belongs to $B(\mathbf{s}, 1/(2\kappa))$. We then apply (17) to get

$$\text{dist}(\mathbf{t}, S) \leq \|\mathbf{t} - \mathbf{s}'\| = \text{dist}(\mathbf{s}', T) \leq \kappa \|\mathbf{t} - \mathbf{s}\|^2.$$

□

We need a bound on the angle between tangent subspaces on a smooth surface as a function of the distance between the corresponding points of contact. This could be deduced directly from (Niyogi et al., 2008, Prop. 6.2, 6.3), but the resulting bound is much looser — and the underlying proof much more complicated — than the following, which is again based on (Federer, 1959, Th. 4.18(2)).

Lemma 2. For $S \in \mathcal{S}_d(\kappa)$, and any $\mathbf{s}, \mathbf{s}' \in S$,

$$\theta_{\max}(T_S(\mathbf{s}), T_S(\mathbf{s}')) \leq 2 \text{asin} \left(\frac{\kappa}{2} \|\mathbf{s}' - \mathbf{s}\| \wedge 1 \right). \quad (20)$$

Proof. By (19) applied twice, we have

$$\text{dist}(\mathbf{s}' - \mathbf{s}, T_S(\mathbf{s})) \vee \text{dist}(\mathbf{s} - \mathbf{s}', T_S(\mathbf{s}')) \leq \frac{\kappa}{2} \|\mathbf{s}' - \mathbf{s}\|^2.$$

Noting that

$$\text{dist}(\mathbf{v}, T) = \|\mathbf{v}\| \sin \angle(\mathbf{v}, T), \quad (21)$$

for any vector \mathbf{v} and any linear subspace T , we get

$$\sin \angle(\mathbf{s}' - \mathbf{s}, T_S(\mathbf{s})) \vee \sin \angle(\mathbf{s}' - \mathbf{s}, T_S(\mathbf{s}')) \leq \frac{\kappa}{2} \|\mathbf{s}' - \mathbf{s}\|.$$

Noting that the LHS never exceeds 1, and applying the arcsine function — which is increasing — on both sides, yields

$$\angle(\mathbf{s}' - \mathbf{s}, T_S(\mathbf{s})) \vee \angle(\mathbf{s}' - \mathbf{s}, T_S(\mathbf{s}')) \leq \text{asin} \left(\frac{\kappa}{2} \|\mathbf{s}' - \mathbf{s}\| \wedge 1 \right).$$

We then use the triangle inequality

$$\theta_{\max}(T_S(\mathbf{s}), T_S(\mathbf{s}')) \leq \angle(\mathbf{s}' - \mathbf{s}, T_S(\mathbf{s})) + \angle(\mathbf{s}' - \mathbf{s}, T_S(\mathbf{s}')),$$

and conclude. □

Below we state some properties of a projection onto a tangent subspace. A result similar to the first part was proved in (Arias-Castro et al., 2011, Lem. 2) based on results in (Niyogi et al., 2008), but the arguments are simpler here and the constants are sharper.

Lemma 3. *Take $S \in \mathcal{S}_d(\kappa)$, $\mathbf{s} \in S$ and $r \leq \frac{1}{2\kappa}$, and let T be short for $T_S(\mathbf{s})$. P_T is injective on $B(\mathbf{s}, r) \cap S$ and its image contains $B(\mathbf{s}, r') \cap T$, where $r' := (1 - \frac{1}{2}(\kappa r)^2)r$. Moreover, P_T^{-1} has Lipschitz constant bounded by $1 + \frac{64}{49}(\kappa r)^2$ over $B(\mathbf{s}, r) \cap T$, for any $r \leq \frac{7}{16\kappa}$.*

Proof. Take $\mathbf{s}', \mathbf{s}'' \in S$ distinct such that $P_T(\mathbf{s}') = P_T(\mathbf{s}'')$. Equivalently, $\mathbf{s}'' - \mathbf{s}'$ is perpendicular to $T_S(\mathbf{s})$. Let T' be short for $T_S(\mathbf{s}')$. By (19) and (21), we have

$$\angle(\mathbf{s}'' - \mathbf{s}', T') \leq \text{asin}\left(\frac{\kappa}{2}\|\mathbf{s}'' - \mathbf{s}'\| \wedge 1\right),$$

and by (20),

$$\theta_{\max}(T, T') \leq 2 \text{asin}\left(\frac{\kappa}{2}\|\mathbf{s}' - \mathbf{s}\| \wedge 1\right).$$

Now, by the triangle inequality,

$$\angle(\mathbf{s}'' - \mathbf{s}', T) \geq \angle(\mathbf{s}'' - \mathbf{s}', T') - \theta_{\max}(T, T') = \frac{\pi}{2} - \theta_{\max}(T, T'),$$

so that

$$\text{asin}\left(\frac{\kappa}{2}\|\mathbf{s}'' - \mathbf{s}'\| \wedge 1\right) \geq \frac{\pi}{2} - 2 \text{asin}\left(\frac{\kappa}{2}\|\mathbf{s}' - \mathbf{s}\| \wedge 1\right).$$

When $\|\mathbf{s}' - \mathbf{s}\| \leq 1/\kappa$, the RHS is bounded from below by $\pi/2 - 2 \text{asin}(1/2)$, which then implies that $\frac{\kappa}{2}\|\mathbf{s}'' - \mathbf{s}'\| \geq \sin(\pi/2 - 2 \text{asin}(1/2)) = 1/2$, that is, $\|\mathbf{s}'' - \mathbf{s}'\| \geq 1/\kappa$. This precludes the situation where $\mathbf{s}', \mathbf{s}'' \in B(\mathbf{s}, 1/(2\kappa))$, so that P_T is injective on $B(\mathbf{s}, r)$ when $r \leq 1/(2\kappa)$.

The same arguments imply that P_T is an open map on $R := B(\mathbf{s}, r) \cap S$. In particular, $P_T(R)$ contains an open ball in T centered at \mathbf{s} and $P_T(\partial R) = \partial P_T(R)$, with $\partial R = S \cap \partial B(\mathbf{s}, r)$ since $\partial S = \emptyset$. Now take any ray out of \mathbf{s} within T , which is necessarily of the form $\mathbf{s} + \mathbb{R}\mathbf{v}$, where \mathbf{v} is a unit vector in T . Let $\mathbf{t}_a = \mathbf{s} + a\mathbf{v} \in T$ for $a \in [0, \infty)$. Let a_* be the infimum over all $a > 0$ such that $\mathbf{t}_a \in P_T(R)$. Note that $a_* > 0$ and $\mathbf{t}_{a_*} \in P_T(\partial R)$, so that there is $\mathbf{s}_* \in \partial R$ such that $P_T(\mathbf{s}_*) = \mathbf{t}_{a_*}$. Let $\mathbf{s}(a) = P_T^{-1}(\mathbf{s} + a\mathbf{v})$, which is well-defined on $[0, a_*]$ by definition of a_* and the fact that P_T is injective on R . We have that $\dot{\mathbf{s}}(a) = D_{\mathbf{t}_a} P_T^{-1} \mathbf{v}$ is the unique vector in $T_a := T_S(P_T^{-1}(\mathbf{t}_a))$ such that $P_T(\dot{\mathbf{s}}(a)) = \mathbf{v}$. Elementary geometry shows that

$$\|P_T(\dot{\mathbf{s}}(a))\| = \|\dot{\mathbf{s}}(a)\| \cos \angle(\dot{\mathbf{s}}(a), T) \geq \|\dot{\mathbf{s}}(a)\| \cos \theta_{\max}(T_a, T),$$

with

$$\cos \theta_{\max}(T_a, T) \geq \cos \left[2 \text{asin} \left(\frac{\kappa}{2} \|\mathbf{s}(a) - \mathbf{s}\| \right) \right] \geq \zeta := 1 - \frac{1}{2}(\kappa r)^2,$$

by (20), $\|\mathbf{s}(a) - \mathbf{s}\| \leq r$ and $\cos[2 \text{asin}(x)] = 1 - 2x^2$ when $0 \leq x \leq 1$. Since $\|P_T(\dot{\mathbf{s}}(a))\| = \|\mathbf{v}\| = 1$, we have $\|\dot{\mathbf{s}}(a)\| \leq 1/\zeta$, and this holds for all $a < a_*$. So we can extend $\mathbf{s}(a)$ to $[0, a_*]$ into a Lipschitz function with constant $1/\zeta$. Together with the fact that $\mathbf{s}_* \in \partial B(\mathbf{s}, r)$, this implies that

$$r = \|\mathbf{s}_* - \mathbf{s}\| = \|\mathbf{s}(a_*) - \mathbf{s}(0)\| \leq \frac{1}{\zeta} \|a_* \mathbf{v}\| = \frac{a_*}{\zeta}.$$

Hence, $a_* \geq \zeta r$ and therefore $P_T(R)$ contains $B(\mathbf{s}, \zeta r) \cap T$ as stated.

For the last part, fix $r < \frac{7}{16}\kappa$, so there is a unique $h < 1/(2\kappa)$ such that $\zeta h = r$, where ζ is redefined as $\zeta := 1 - \frac{1}{2}(\kappa h)^2$. Take $\mathbf{t}' \in B(\mathbf{s}, r) \cap T$ and let $\mathbf{s}' = P_T^{-1}(\mathbf{t}')$ and $T' = T_S(\mathbf{s}')$. We saw that P_T^{-1} is Lipschitz with constant $1/\zeta$ on any ray from \mathbf{s} of length r , so that $\|\mathbf{s}' - \mathbf{s}\| \leq$

$(1/\zeta)\|\mathbf{t}' - \mathbf{s}\| \leq r/\zeta = h$. The differential of P_T at \mathbf{s}' is P_T itself, seen as a linear map between T' and T . Then for any vector $\mathbf{u} \in T'$, we have

$$\|P_T(\mathbf{u})\| = \|\mathbf{u}\| \cos \angle(\mathbf{u}, T) \geq \|\mathbf{u}\| \cos \theta_{\max}(T', T),$$

with

$$\cos \theta_{\max}(T', T) \geq \cos \left[2 \operatorname{asin} \left(\frac{\kappa}{2} \|\mathbf{s}' - \mathbf{s}\| \right) \right] \geq 1 - \frac{1}{2}(\kappa h)^2 = \zeta,$$

as before. Hence, $\|D_{\mathbf{t}'} P_T^{-1}\| \leq 1/\zeta$, and we proved this for all $\mathbf{t}' \in B(\mathbf{s}, r) \cap T$. Since that set is convex, we can apply Taylor's theorem and get that P_T^{-1} is Lipschitz on that set with constant $1/\zeta$. We then have

$$1/\zeta \leq 1 + (\kappa h)^2 \leq 1 + \frac{64}{49}(\kappa r)^2,$$

because $\kappa h \leq 1/2$ and $r = \zeta h \geq 7h/8$. □

6.1.2 Volumes and uniform distributions

Below is a result that quantifies how much the volume of a set changes when applying a Lipschitz map. This is well-known in measure theory and we only provide a proof for completeness.

Lemma 4. *Suppose Ω is a measurable subset of \mathbb{R}^D and $f : \Omega \subset \mathbb{R}^D \rightarrow \mathbb{R}^D$ is C -Lipschitz. Then for any measurable set $A \subset \Omega$ and real $d > 0$, $\operatorname{vol}_d(f(A)) \leq C^d \operatorname{vol}_d(A)$.*

Proof. By definition,

$$\operatorname{vol}_d(A) = \lim_{t \rightarrow 0} V_d^t(A), \quad V_d^t(A) := \inf_{(R_i) \in \mathcal{R}^t(A)} \sum_{i \in \mathbb{N}} \operatorname{diam}(R_i)^d,$$

where $\mathcal{R}^t(A)$ is the class of countable sequences $(R_i : i \in \mathbb{N})$ of subsets of \mathbb{R}^D such that $A \subset \bigcup_i R_i$ and $\operatorname{diam}(R_i) < t$ for all i . Since f is C -Lipschitz, $\operatorname{diam}(f(R)) \leq C \operatorname{diam}(R)$ for any $R \subset \Omega$. Hence, for any $(R_i) \in \mathcal{R}^t(A)$, $(f(R_i)) \in \mathcal{R}^{Ct}(f(A))$. This implies that

$$V_d^{Ct}(f(A)) \leq \sum_{i \in \mathbb{N}} \operatorname{diam}(f(R_i))^d \leq C^d \sum_{i \in \mathbb{N}} \operatorname{diam}(R_i)^d.$$

Taking the infimum over $(R_i) \in \mathcal{R}^t(A)$, we get $V_d^{Ct}(f(A)) \leq C^d V_d^t(A)$, and we conclude by taking the limit as $t \rightarrow 0$, noticing that $V_d^{Ct}(f(A)) \rightarrow \operatorname{vol}(f(A))$. □

We compare below two uniform distributions. For two Borel probability measures P and Q on \mathbb{R}^D , $\operatorname{TV}(P, Q)$ denotes their total variation distance, meaning,

$$\operatorname{TV}(P, Q) = \sup\{|P(A) - Q(A)| : A \text{ Borel set}\}.$$

Remember that for a Borel set A , λ_A denotes the uniform distribution on A .

Lemma 5. *Suppose A and B are two Borel subsets of \mathbb{R}^D . Then*

$$\operatorname{TV}(\lambda_A, \lambda_B) \leq 4 \frac{\operatorname{vol}(A \triangle B)}{\operatorname{vol}(A \cup B)}.$$

Proof. If A and B are not of same dimension, say $\dim(A) > \dim(B)$, then $\text{TV}(\lambda_A, \lambda_B) = 1$ since $\lambda_A(B) = 0$ while $\lambda_B(B) = 1$. And we also have

$$\text{vol}(A \triangle B) = \text{vol}_{\dim(A)}(A \triangle B) = \text{vol}_{\dim(A)}(A) = \text{vol}(A),$$

and

$$\text{vol}(A \cup B) = \text{vol}_{\dim(A)}(A \cup B) = \text{vol}_{\dim(A)}(A) = \text{vol}(A),$$

in both cases because $\text{vol}_{\dim(A)}(B) = 0$. So the result works in that case.

Therefore assume that A and B are of same dimension. Assume WLOG that $\text{vol}(A) \geq \text{vol}(B)$. For any Borel set U ,

$$\lambda_A(U) - \lambda_B(U) = \frac{\text{vol}(A \cap U)}{\text{vol}(A)} - \frac{\text{vol}(B \cap U)}{\text{vol}(B)},$$

so that

$$\begin{aligned} |\lambda_A(U) - \lambda_B(U)| &\leq \frac{|\text{vol}(A \cap U) - \text{vol}(B \cap U)|}{\text{vol}(A)} + \text{vol}(B \cap U) \left| \frac{1}{\text{vol}(A)} - \frac{1}{\text{vol}(B)} \right| \\ &\leq \frac{\text{vol}(A \triangle B)}{\text{vol}(A)} + \frac{\text{vol}(B \cap U)}{\text{vol}(B)} \frac{|\text{vol}(A) - \text{vol}(B)|}{\text{vol}(A)} \\ &\leq \frac{2 \text{vol}(A \triangle B)}{\text{vol}(A)}, \end{aligned}$$

and we conclude with the fact that $\text{vol}(A \cup B) \leq \text{vol}(A) + \text{vol}(B) \leq 2 \text{vol}(A)$. \square

We now look at the projection of the uniform distribution on a neighborhood of a surface onto a tangent subspace. For a Borel probability measure P and measurable function $f : \mathbb{R}^D \rightarrow \mathbb{R}^D$, P^f denotes the push-forward (Borel) measure defined by $P^f(A) = P(f^{-1}(A))$.

Lemma 6. *Suppose $A \subset \mathbb{R}^D$ is Borel and $f : A \rightarrow \mathbb{R}^D$ is invertible on $f(A)$, and that both f and f^{-1} are C -Lipschitz. Then*

$$\text{TV}(\lambda_A^f, \lambda_{f(A)}) \leq 8(C^{\dim(A)} - 1).$$

Proof. First, note that A and $f(A)$ are both of same dimension, and that $C \geq 1$ necessarily. Let d be short for $\dim(A)$. Take $U \subset f(A)$ Borel and let $V = f^{-1}(U)$. Then

$$\lambda_A^f(U) = \frac{\text{vol}(A \cap V)}{\text{vol}(A)}, \quad \lambda_{f(A)}(U) = \frac{\text{vol}(f(A) \cap U)}{\text{vol}(f(A))},$$

$$|\lambda_A^f(U) - \lambda_{f(A)}(U)| \leq \frac{|\text{vol}(A \cap V) - \text{vol}(f(A) \cap U)|}{\text{vol}(A)} + \frac{|\text{vol}(A) - \text{vol}(f(A))|}{\text{vol}(A)}.$$

f being invertible, we have $f(A \cap V) = f(A) \cap U$ and $f^{-1}(f(A) \cap U) = A \cap V$. Therefore, applying Lemma 4, we get

$$C^{-d} \leq \frac{\text{vol}(f(A) \cap U)}{\text{vol}(A \cap V)} \leq C^d,$$

so that

$$|\text{vol}(A \cap V) - \text{vol}(f(A) \cap U)| \leq (C^d - 1) \text{vol}(A \cap V) \leq (C^d - 1) \text{vol}(A).$$

Similarly,

$$|\text{vol}(A) - \text{vol}(f(A))| \leq (C^d - 1) \text{vol}(A).$$

We then conclude with Lemma 5. \square

Now comes a technical result on the intersection of a smooth surface and a ball.

Lemma 7. *There is a constant $C_7 \geq 3$ depending only on d such that the following is true. Take $S \in \mathcal{S}_d(\kappa)$, $r < \frac{1}{C_7\kappa}$ and $\mathbf{x} \in \mathbb{R}^D$ such that $\text{dist}(\mathbf{x}, S) < r$. Let $\mathbf{s} = P_S(\mathbf{x})$ and $T = T_S(\mathbf{s})$. Then*

$$\text{vol}(P_T(S \cap B(\mathbf{x}, r)) \triangle (T \cap B(\mathbf{x}, r))) \leq C_7(\|\mathbf{x} - \mathbf{s}\| + r^2) \text{vol}(T \cap B(\mathbf{x}, r)).$$

Proof. Let $A_r = B(\mathbf{s}, r)$, $B_r = B(\mathbf{x}, r)$ and $g = P_T$ for short. Note that $T \cap B_r = T \cap A_{r_0}$ where $r_0 := (r^2 - \delta^2)^{1/2}$ and $\delta := \|\mathbf{x} - \mathbf{s}\|$. Take $\mathbf{s}_1 \in S \cap B_r$ such that $g(\mathbf{s}_1)$ is farthest from \mathbf{s} , so that $g(S \cap B_r) \subset A_{r_1}$ where $r_1 := \|\mathbf{s} - g(\mathbf{s}_1)\|$ — note that $r_1 \leq r$. Let $\ell_1 = \|\mathbf{s}_1 - g(\mathbf{s}_1)\|$ and \mathbf{y}_1 be the orthogonal projection of \mathbf{s}_1 onto the line (\mathbf{x}, \mathbf{s}) . By Pythagoras theorem, we have $\|\mathbf{x} - \mathbf{s}_1\|^2 = \|\mathbf{x} - \mathbf{y}_1\|^2 + \|\mathbf{y}_1 - \mathbf{s}_1\|^2$. We have $\|\mathbf{x} - \mathbf{s}_1\| \leq r$ and $\|\mathbf{y}_1 - \mathbf{s}_1\| = \|\mathbf{s} - g(\mathbf{s}_1)\| = r_1$. And because $\ell_1 \leq \kappa r_1^2 < r$ by (17), either \mathbf{y}_1 is between \mathbf{x} and \mathbf{s} , in which case $\|\mathbf{x} - \mathbf{y}_1\| = \delta - \ell_1$, or \mathbf{s} is between \mathbf{x} and \mathbf{y}_1 , in which case $\|\mathbf{x} - \mathbf{y}_1\| = \delta + \ell_1$. In any case, $r^2 \geq r_1^2 + (\delta - \ell_1)^2$, which together with $\ell_1 \leq \kappa r_1^2$ implies $r_1^2 \leq r^2 - \delta^2 + 2\delta\ell_1 \leq r_0^2 + 2\kappa r_1^2 \delta$, leading to $r_1 \leq (1 - 2\kappa\delta)^{-1/2} r_0 \leq (1 + 4\kappa\delta)r_0$ after noticing that $\delta \leq r < 1/(3\kappa)$. From $g(S \cap B_r) \subset T \cap A_{r_1}$, we get

$$\begin{aligned} \text{vol}(g(S \cap B_r) \setminus (T \cap B_r)) &\leq \text{vol}(T \cap A_{r_1}) - \text{vol}(T \cap A_{r_0}) \\ &= ((r_1/r_0)^d - 1) \text{vol}(T \cap A_{r_0}). \end{aligned}$$

We follow similar arguments to get a sort of reverse relationship. Take $\mathbf{s}_2 \in S \cap B_r$ such that $g(S \cap B_r) \supset T \cap A_{r_2}$, where $r_2 := \|\mathbf{s} - g(\mathbf{s}_2)\|$ is largest. Assuming r is small enough, by Lemma 3, g^{-1} is well-defined on $T \cap A_r$, so that necessarily $\mathbf{s}_2 \in \partial B_r$. Let $\ell_2 = \|\mathbf{s}_2 - g(\mathbf{s}_2)\|$ and \mathbf{y}_2 be the orthogonal projection of \mathbf{s}_2 onto the line (\mathbf{x}, \mathbf{s}) . By Pythagoras theorem, we have $\|\mathbf{x} - \mathbf{s}_2\|^2 = \|\mathbf{x} - \mathbf{y}_2\|^2 + \|\mathbf{y}_2 - \mathbf{s}_2\|^2$. We have $\|\mathbf{x} - \mathbf{s}_2\| = r$ and $\|\mathbf{y}_2 - \mathbf{s}_2\| = \|\mathbf{s} - g(\mathbf{s}_2)\| = r_2$. And by the triangle inequality, $\|\mathbf{x} - \mathbf{y}_2\| \leq \|\mathbf{x} - \mathbf{s}\| + \|\mathbf{y}_2 - \mathbf{s}\| = \delta + \ell_2$. Hence, $r^2 \leq r_2^2 + (\delta + \ell_2)^2$, which together with $\ell_2 \leq \kappa r_2^2$ by (17), implies $r_2^2 \geq r^2 - \delta^2 - 2\delta\ell_2 - \ell_2^2 \geq r_0^2 - (2\delta + \kappa r^2)\kappa r_2^2$, leading to $r_2 \geq (1 + 2\kappa\delta + \kappa^2 r^2)^{-1/2} r_0 \geq (1 - 2\kappa\delta - \kappa^2 r^2)r_0$. From $g(S \cap B_r) \supset T \cap A_{r_2}$, we get

$$\begin{aligned} \text{vol}((T \cap B_r) \setminus g(S \cap B_r)) &\leq \text{vol}(T \cap A_{r_0}) - \text{vol}(T \cap A_{r_2}) \\ &= (1 - (r_2/r_0)^d) \text{vol}(T \cap A_{r_0}). \end{aligned}$$

All together, we have

$$\begin{aligned} \text{vol}(g(S \cap B_r) \triangle (T \cap B_r)) &\leq ((r_1/r_0)^d - (r_2/r_0)^d) \text{vol}(T \cap A_{r_0}) \\ &\leq ((1 + 4\kappa\delta)^d - (1 - 2\kappa\delta - \kappa^2 r^2)^d) \text{vol}((T \cap B_r)), \end{aligned}$$

with $(1 + 4\kappa r)^d - (1 - 4\kappa r)^d \leq C(\delta + r^2)$ when $\delta \leq r \leq 1/(3\kappa)$, for a constant C depending only on d and κ . The result follows from this. \square

We bound below the d -volume of a the intersection of a ball with a smooth surface. Though it could be obtained as a special case of Lemma 7, we provide a direct proof because this result is at the cornerstone of many results in the literature on sampling points uniformly on a smooth surface.

Lemma 8. *Suppose $S \in \mathcal{S}_d(\kappa)$. Then for any $\mathbf{s} \in S$ and $r < \frac{1}{(d\sqrt{3})\kappa}$, we have*

$$1 - 2d\kappa r \leq \frac{\text{vol}(S \cap B(\mathbf{s}, r))}{\text{vol}(T \cap B(\mathbf{s}, r))} \leq 1 + 2d\kappa r,$$

where $T := T_S(\mathbf{s})$ is the tangent subspace of S at \mathbf{s} .

Proof. Let $T = T_S(\mathbf{s})$, $B_r = B(\mathbf{s}, r)$ and $g = P_T$ for short. By Lemma 3, g is bi-Lipschitz with constants $(1 + \kappa r)^{-1}$ and 1 on $S \cap B_r$, so by Lemma 4 we have

$$(1 + \kappa r)^{-d} \leq \frac{\text{vol}(g(S \cap B_r))}{\text{vol}(S \cap B_r)} \leq 1.$$

That g^{-1} is Lipschitz with constant $1 + \kappa r$ on $g(S \cap B_r)$ also implies that $g(S \cap B_r)$ contains $T \cap B_{r'}$ where $r' := r/(1 + \kappa r)$. From this, and the fact that $g(S \cap B_r) \subset T \cap B_r$, we get

$$1 \leq \frac{\text{vol}(T \cap B_r)}{\text{vol}(g(S \cap B_r))} \leq \frac{\text{vol}(T \cap B_r)}{\text{vol}(T \cap B_{r'})} = \frac{r^d}{r'^d} = (1 + \kappa r)^d. \quad (22)$$

We therefore have

$$\text{vol}(S \cap B_r) \geq \text{vol}(g(S \cap B_r)) \geq (1 + \kappa r)^{-d} \text{vol}(T \cap B_r),$$

and

$$\text{vol}(S \cap B_r) \leq (1 + \kappa r)^d \text{vol}(g(S \cap B_r)) \leq (1 + \kappa r)^d \text{vol}(T \cap B_r).$$

And we conclude with the inequality $(1 + x)^d \leq 1 + 2dx$ valid for any $x \in [0, 1/d]$ and any $d \geq 1$. \square

We now look at the density of a sample from the uniform on a smooth, compact surface.

Lemma 9. *There is a constant $C_9 > 0$ such that the following is true. If $S \in \mathcal{S}_d(\kappa)$ and we sample n points $\mathbf{s}_1, \dots, \mathbf{s}_n$ independently and uniformly at random from S , and if $0 < r < 1/(C_9\kappa)$, then with probability at least $1 - C_9 r^{-d} \exp(-nr^d/C_9)$, any ball of radius r with center on S has between nr^d/C_9 and $C_9 nr^d$ sample points.*

Proof. For a set R , let $N(R)$ denote the number of sample points in R . For any R measurable, $N(R) \sim \text{Bin}(n, p_R)$, where $p_R := \text{vol}(R \cap S)/\text{vol}(S)$. Let $\mathbf{x}_1, \dots, \mathbf{x}_m$ be an $(r/2)$ -packing of S , and let $B_i = B(\mathbf{x}_i, r/4) \cap S$. For any $\mathbf{s} \in S$, there is j such that $\|\mathbf{s} - \mathbf{x}_j\| \leq r/2$, which implies $B_i \subset B(\mathbf{s}, r)$ by the triangle inequality. Hence, $\min_{\mathbf{s} \in S} N(B(\mathbf{s}, r)) \geq \min_i N(B_i)$.

By the fact that $B_i \cap B_j = \emptyset$ for $i \neq j$,

$$\text{vol}(S) \geq \sum_{i=1}^m \text{vol}(B_i) \geq m \min_i \text{vol}(B_i),$$

and assuming that r is small enough that we may apply Lemma 8, we have

$$\min_i \text{vol}(B_i) \geq \frac{\omega_d}{2} (r/4)^d,$$

where ω_d is the volume of the d -dimensional unit ball. This leads to $m \leq Cr^{-d}$ and $p := \min_i p_{B_i} \geq r^d/C$, where $C > 0$ depends only on S .

Now, applying Bernstein's inequality to the binomial distribution, we get

$$\mathbb{P}(N(B_i) \leq np/2) \leq \mathbb{P}(N(B_i) \leq np_{B_i}/2) \leq e^{-(3/32)np_{B_i}} \leq e^{-(3/32)np}. \quad (23)$$

We follow this with the union bound, to get

$$\mathbb{P}\left(\min_{\mathbf{s} \in S} N(B(\mathbf{s}, r)) \leq nr^d/(2C)\right) \leq m e^{-(3/32)np} \leq Cr^{-d} e^{-\frac{3}{32C}nr^d}.$$

From this the lower bound follows. The proof of the upper bound is similar. \square

Next, we bound the volume of the symmetric difference between two balls.

Lemma 10. *Take $\mathbf{x}, \mathbf{y} \in \mathbb{R}^d$ and $0 < \delta \leq 1$. Then*

$$\frac{\text{vol}(B(\mathbf{x}, \delta) \triangle B(\mathbf{y}, 1))}{2 \text{vol}(B(0, 1))} \leq 1 - (1 - \|\mathbf{x} - \mathbf{y}\|)_+^d \wedge \delta^d.$$

Proof. It suffices to prove the result when $\|\mathbf{x} - \mathbf{y}\| < 1$. In that case, with $\gamma := (1 - \|\mathbf{x} - \mathbf{y}\|) \wedge \delta$, we have $B(\mathbf{x}, \gamma) \subset B(\mathbf{x}, \delta) \cap B(\mathbf{y}, 1)$, so that

$$\begin{aligned} \text{vol}(B(\mathbf{x}, \delta) \triangle B(\mathbf{y}, 1)) &= \text{vol}(B(\mathbf{x}, \delta)) + \text{vol}(B(\mathbf{y}, 1)) - 2 \text{vol}(B(\mathbf{x}, \delta) \cap B(\mathbf{y}, 1)) \\ &\leq 2 \text{vol}(B(\mathbf{y}, 1)) - 2 \text{vol}(B(\mathbf{x}, \gamma)) \\ &= 2 \text{vol}(B(\mathbf{y}, 1))(1 - \gamma^d). \end{aligned}$$

□

6.1.3 Covariances

The result below describes explicitly the covariance matrix of the uniform distribution over the unit ball of a subspace.

Lemma 11. *Let T be a subspace of dimension d . Then the covariance matrix of the uniform distribution on $T \cap B(0, 1)$ (seen as a linear map) is equal to cP_T , where $c := \frac{1}{d+2}$.*

Proof. Assume WLOG that $T = \mathbb{R}^d \times \{0\}$. Let X be distributed according to the uniform distribution on $T \cap B(0, 1)$ and let $R = \|X\|$. Note that

$$\mathbb{P}(R \leq r) = \frac{\text{vol}(T \cap B(0, r))}{\text{vol}(T \cap B(0, 1))} = r^d, \quad \forall r \in [0, 1].$$

By symmetry, $\mathbb{E}(X_i X_j) = 0$ if $i \neq j$, while

$$\mathbb{E}(X_1^2) = \frac{1}{d} \mathbb{E}(X_1^2 + \dots + X_d^2) = \frac{1}{d} \mathbb{E}(R^2) = \frac{1}{d} \int_0^1 r^2 \cdot dr^{d-1} dr = \frac{1}{d+2}.$$

This is exactly the representation of $\frac{1}{d+2}P_T$ in the canonical basis of \mathbb{R}^D . □

We now show that a bound on the total variation distance between two compactly supported distributions implies a bound on the difference between their covariance matrices. For a measure P on \mathbb{R}^D and an integrable function f , let $P(f)$ denote the integral of f with respect to P , that is,

$$P(f) = \int f(x)P(dx),$$

and let $\mathbb{E}(P) = P(\mathbf{x})$ and $\text{Cov}(P) = P(\mathbf{x}\mathbf{x}^\top) - P(\mathbf{x})P(\mathbf{x})^\top$ denote the mean and covariance matrix of P , respectively.

Lemma 12. *Suppose λ and ν are two Borel probability measures on \mathbb{R}^d supported on $B(0, 1)$. Then*

$$\|\mathbb{E}(\lambda) - \mathbb{E}(\nu)\| \leq \sqrt{d} \text{TV}(\lambda, \nu), \quad \|\text{Cov}(\lambda) - \text{Cov}(\nu)\| \leq 3d \text{TV}(\lambda, \nu).$$

Proof. Let $f_k(\mathbf{t}) = t_k$ when $\mathbf{t} = (t_1, \dots, t_d)$, and note that $|f_k(\mathbf{t})| \leq 1$ for all k and all $\mathbf{t} \in B(0, 1)$. By the fact that

$$\text{TV}(\lambda, \nu) = \sup\{\lambda(f) - \nu(f) : f : \mathbb{R}^d \rightarrow \mathbb{R} \text{ measurable with } |f| \leq 1\},$$

we have

$$|\lambda(f_k) - \nu(f_k)| \leq \text{TV}(\lambda, \nu), \quad \forall k = 1, \dots, d.$$

Therefore,

$$\|\mathbb{E}(\lambda) - \mathbb{E}(\nu)\|^2 = \sum_{k=1}^d (\lambda(f_k) - \nu(f_k))^2 \leq d \text{TV}(\lambda, \nu)^2,$$

which proves the first part.

Similarly, let $f_{k\ell}(\mathbf{t}) = t_k t_\ell$. Since $|f_{k\ell}(\mathbf{t})| \leq 1$ for all k, ℓ and all $\mathbf{t} \in B(0, 1)$, we have

$$|\lambda(f_{k\ell}) - \nu(f_{k\ell})| \leq \text{TV}(\lambda, \nu), \quad \forall k, \ell = 1, \dots, d.$$

Since for any probability measure μ on \mathbb{R}^d ,

$$\text{Cov}(\mu) = (\mu(f_{k\ell}) - \mu(f_k)\mu(f_\ell) : k, \ell = 1, \dots, d),$$

we have

$$\begin{aligned} \|\text{Cov}(\lambda) - \text{Cov}(\nu)\| &\leq d \max_{k,\ell} (|\lambda(f_{k\ell}) - \nu(f_{k\ell})| + |\lambda(f_k)\lambda(f_\ell) - \nu(f_k)\nu(f_\ell)|) \\ &\leq d \max_{k,\ell} (|\lambda(f_{k\ell}) - \nu(f_{k\ell})| + |\lambda(f_k)||\lambda(f_\ell) - \nu(f_\ell)| + |\nu(f_\ell)||\lambda(f_k) - \nu(f_k)|) \\ &\leq 3d \text{TV}(\lambda, \nu), \end{aligned}$$

using the fact that $|\lambda(f_k)| \leq 1$ and $|\nu(f_k)| \leq 1$ for all k . \square

Next we compare the covariance matrix of the uniform distribution on a small piece of smooth surface with that of the uniform distribution on the projection of that piece onto a nearby tangent subspace.

Lemma 13. *There is a constant $C_{13} > 0$ depending only on d such that the following is true. Take $S \in \mathcal{S}_d(\kappa)$, $r < \frac{1}{C_{13}\kappa}$ and $\mathbf{x} \in \mathbb{R}^D$ such that $\text{dist}(\mathbf{x}, S) \leq r$. Let $\mathbf{s} = P_S(\mathbf{x})$ and $T = T_S(\mathbf{s})$. If $\boldsymbol{\zeta}$ and $\boldsymbol{\xi}$ are the means, and \mathbf{M} and \mathbf{N} are the covariance matrices of the uniform distributions on $S \cap B(\mathbf{x}, r)$ and $T \cap B(\mathbf{x}, r)$ respectively, then*

$$\|\boldsymbol{\zeta} - \boldsymbol{\xi}\| \leq C_{13}\kappa r^2, \quad \|\mathbf{M} - \mathbf{N}\| \leq C_{13}\kappa r^3.$$

Proof. We focus on proving the bound on the covariances, and leave the bound on the means — whose proof is both similar and simpler — as an exercise to the reader. Let $T = T_S(\mathbf{s})$, $B_r = B(\mathbf{x}, r)$ and $g = P_T$ for short. Let $A = S \cap B_r$ and $A' = T \cap B_r$. Let $X \sim \lambda_A$ and define $Y = g(X)$ with distribution denoted $\lambda_{A'}^g$. We have

$$\text{Cov}(X) - \text{Cov}(Y) = \frac{1}{2}(\text{Cov}(X - Y, X + Y) + \text{Cov}(X + Y, X - Y)),$$

where $\text{Cov}(U, V) = \mathbb{E}((U - \boldsymbol{\mu}_U)(V - \boldsymbol{\mu}_V)^T)$ is the cross-covariance of random vectors U and V with respective means $\boldsymbol{\mu}_U$ and $\boldsymbol{\mu}_V$. Note that by Jensen's inequality, the fact $\|\mathbf{u}\mathbf{v}^T\| = \|\mathbf{u}\|\|\mathbf{v}\|$ for any pair of vectors \mathbf{u}, \mathbf{v} , and then the Cauchy-Schwarz inequality

$$\|\text{Cov}(U, V)\| \leq \mathbb{E}(\|U - \boldsymbol{\mu}_U\| \cdot \|V - \boldsymbol{\mu}_V\|) \leq \mathbb{E}(\|U - \boldsymbol{\mu}_U\|^2)^{1/2} \cdot \mathbb{E}(\|V - \boldsymbol{\mu}_V\|^2)^{1/2}.$$

Hence, letting $\boldsymbol{\mu}_X = \mathbb{E}X$ and $\boldsymbol{\mu}_Y = \mathbb{E}Y$, we have

$$\begin{aligned}
\|\text{Cov}(\lambda_A) - \text{Cov}(\lambda_A^g)\| &\leq \|\text{Cov}(X - Y, X + Y)\| \\
&\leq \mathbb{E}[\|X - Y - \boldsymbol{\mu}_X + \boldsymbol{\mu}_Y\|^2]^{1/2} \mathbb{E}[\|X + Y - \boldsymbol{\mu}_X - \boldsymbol{\mu}_Y\|^2]^{1/2} \\
&\leq \mathbb{E}[\|X - Y\|^2]^{1/2} \left(\mathbb{E}[\|X - \mathbf{s}\|^2]^{1/2} + \mathbb{E}[\|Y - \mathbf{s}\|^2]^{1/2} \right) \\
&\leq \frac{\kappa}{2} r^2 (r + r) = \kappa r^3,
\end{aligned} \tag{24}$$

where the third inequality is due to the triangle inequality and fact that the mean minimizes the mean-squared error, and the third to the fact that $X, Y \in B_r$ and (16).

Assume $r < 1/((C_7 \vee d)\kappa)$. Let $\lambda_{g(A)}$ denote the uniform distribution on $g(A)$. λ_A^g and $\lambda_{g(A)}$ are both supported on B_r , so that applying Lemma 12 with proper scaling, we get

$$\|\text{Cov}(\lambda_A^g) - \text{Cov}(\lambda_{g(A)})\| \leq 3dr^2 \text{TV}(\lambda_A^g, \lambda_{g(A)}).$$

We know that g is 1-Lipschitz, and by Lemma 3 — which is applicable since $C_7 \geq 3$ — g^{-1} is well-defined and is $(1 + \kappa r)$ -Lipschitz on B_r . Hence, by Lemma 6 and the fact that $\dim(A) = d$, we have

$$\text{TV}(\lambda_A^g, \lambda_{g(A)}) \leq 8((1 + \kappa r)^d - 1) \leq 16d\kappa r,$$

using the inequality $(1 + x)^d \leq 1 + 2dx$, valid for any $x \in [0, 1/d]$ and any $d \geq 1$.

Noting that $\lambda_{A'}$ is also supported on B_r , applying Lemma 12 with proper scaling, we get

$$\|\text{Cov}(\lambda_{g(A)}) - \text{Cov}(\lambda_{A'})\| \leq 3dr^2 \text{TV}(\lambda_{g(A)}, \lambda_{A'}),$$

with

$$\text{TV}(\lambda_{g(A)}, \lambda_{A'}) \leq 4 \frac{\text{vol}(A \triangle A')}{\text{vol}(A')} \leq C\kappa r,$$

by Lemma 5 and Lemma 7, where C depends only on d, κ .

By the triangle inequality,

$$\begin{aligned}
\|\mathbf{M} - \mathbf{N}\| &= \|\text{Cov}(\lambda_A) - \text{Cov}(\lambda_{A'})\| \\
&\leq \|\text{Cov}(\lambda_A) - \text{Cov}(\lambda_A^g)\| + \|\text{Cov}(\lambda_A^g) - \text{Cov}(\lambda_{g(A)})\| + \|\text{Cov}(\lambda_{g(A)}) - \text{Cov}(\lambda_{A'})\| \\
&\leq \kappa r^3 + 48d^2 \kappa r^3 + Cr^3.
\end{aligned}$$

From this, we conclude. □

Next is a lemma on the estimation of a covariance matrix. The result is a simple consequence of the matrix Hoeffding inequality of Tropp (2012). Note that simply bounding the operator norm by the Frobenius norm, and then applying the classical Hoeffding inequality (Hoeffding, 1963) would yield a bound sufficient for our purposes, but this is a good opportunity to use a more recent and sophisticated result.

Lemma 14. *Let \mathbf{C}_m denote the empirical covariance matrix based on an i.i.d. sample of size m from a distribution on the unit ball of \mathbb{R}^d with covariance $\boldsymbol{\Sigma}$. Then*

$$\mathbb{P}(\|\mathbf{C}_m - \boldsymbol{\Sigma}\| > t) \leq 4d \exp\left(-\frac{mt}{16} \min\left(\frac{t}{32}, \frac{m}{d}\right)\right).$$

Proof. Without loss of generality, we assume that the distribution has zero mean and is now supported on $B(0, 2)$. Let $\mathbf{x}_1, \dots, \mathbf{x}_m$ denote the sample, with $\mathbf{x}_i = (x_{i,1}, \dots, x_{i,d})$. We have

$$\mathbf{C}_m = \mathbf{C}_m^* - \frac{1}{m} \bar{\mathbf{x}} \bar{\mathbf{x}}^T,$$

where

$$\mathbf{C}_m^* := \frac{1}{m} \sum_{i=1}^m \mathbf{x}_i \mathbf{x}_i^T, \quad \bar{\mathbf{x}} := \frac{1}{m} \sum_{i=1}^m \mathbf{x}_i.$$

Note that

$$\|\mathbf{C}_m - \Sigma\| \leq \|\mathbf{C}_m^* - \Sigma\| + \frac{1}{m} \|\bar{\mathbf{x}}\|^2.$$

Applying the union bound and then Hoeffding's inequality to each coordinate — which is in $[-2, 2]$ — we get

$$\mathbb{P}(\|\bar{\mathbf{x}}\| > t) \leq \sum_{j=1}^d \mathbb{P}(|\bar{x}_j| > t/\sqrt{d}) \leq 2d \exp\left(-\frac{mt^2}{8d}\right).$$

Noting that $\frac{1}{m}(\mathbf{x}_i \mathbf{x}_i^T - \Sigma)$, $i = 1, \dots, m$, are independent, zero-mean, self-adjoint matrices with spectral norm bounded by $4/m$, we may apply the matrix Hoeffding inequality ([Tropp, 2012](#), Th. 1.3), we get

$$\mathbb{P}(\|\mathbf{C}_m^* - \Sigma\| > t) \leq 2d \exp\left(-\frac{t^2}{8\sigma^2}\right), \quad \sigma^2 := m(4/m)^2 = 16/m.$$

Applying the union bound and using the previous inequalities, we arrive at

$$\begin{aligned} \mathbb{P}(\|\mathbf{C}_m - \Sigma\| > t) &\leq \mathbb{P}(\|\mathbf{C}_m^* - \Sigma\| > t/2) + \mathbb{P}(\|\bar{\mathbf{x}}\| > \sqrt{mt/2}) \\ &\leq 2d \exp\left(-\frac{mt^2}{512}\right) + 2d \exp\left(-\frac{m^2 t}{16d}\right) \\ &\leq 4d \exp\left(-\frac{mt}{16} \min\left(\frac{t}{32}, \frac{m}{d}\right)\right). \end{aligned}$$

□

6.1.4 Projections

We relate below the difference of two orthogonal projections with the largest principal angle between the corresponding subspaces.

Lemma 15. *For two affine non-null subspaces T, T' ,*

$$\|P_T - P_{T'}\| = \begin{cases} \sin \theta_{\max}(T, T'), & \text{if } \dim(T) = \dim(T'), \\ 1, & \text{otherwise.} \end{cases}$$

Proof. For two affine subspaces $T, T' \subset \mathbb{R}^D$ of same dimension, let $\frac{\pi}{2} \geq \theta_1 \geq \dots \geq \theta_D \geq 0$, denote the principal angles between them. By ([Stewart and Sun, 1990](#), Th. I.5.5), the singular values of $P_T - P_{T'}$ are $\{\sin \theta_j : j = 1, \dots, q\}$, so that $\|P_T - P_{T'}\| = \max_j \sin \theta_j = \sin \theta_1 = \sin \theta_{\max}(T, T')$. Suppose now that T and T' are of different dimension, say $\dim(T) > \dim(T')$. We have $\|P_T - P_{T'}\| \leq \|P_T\| \vee \|P_{T'}\| = 1$, since P_T and $P_{T'}$ are orthogonal projections and therefore positive semidefinite with operator norm equal to 1. Let $L = P_T(T')$. Since $\dim(L) \leq \dim(T') < \dim(T)$, there is $\mathbf{u} \in T \cap L^\perp$ with $\mathbf{u} \neq 0$. Then $\mathbf{v}^\top \mathbf{u} = P_T(\mathbf{v})^\top \mathbf{u} = 0$ for all $\mathbf{v} \in T'$, implying that $P_{T'}(\mathbf{u}) = 0$ and consequently $(P_T - P_{T'})\mathbf{u} = \mathbf{u}$, so that $\|P_T - P_{T'}\| \geq 1$. □

The lemma below is a perturbation result for eigenspaces and widely known as the $\sin \Theta$ Theorem of [Davis and Kahan \(1970\)](#). See also ([Luxburg, 2007](#), Th. 7) or ([Stewart and Sun, 1990](#), Th. V.3.6).

Lemma 16 (Davis and Kahan). *Let \mathbf{M} be positive semi-definite with eigenvalues $\beta_1 \geq \beta_2 \geq \dots$. Suppose that $\Delta_d := \beta_d - \beta_{d+1} > 0$. Then for any other positive semi-definite matrix \mathbf{N} ,*

$$\|P_{\mathbf{N}}^{(d)} - P_{\mathbf{M}}^{(d)}\| \leq \frac{\sqrt{2}\|\mathbf{N} - \mathbf{M}\|}{\Delta_d},$$

where $P_{\mathbf{M}}^{(d)}$ and $P_{\mathbf{N}}^{(d)}$ denote the orthogonal projections onto the top d eigenvectors of \mathbf{M} and \mathbf{N} , respectively.

6.1.5 Intersections

We start with an elementary result on points near the intersection of two affine subspaces.

Lemma 17. *Take any two linear subspaces $T_1, T_2 \subset \mathbb{R}^D$. For any point $\mathbf{t}_1 \in T_1 \setminus T_2$, we have*

$$\text{dist}(\mathbf{t}_1, T_2) \geq \text{dist}(\mathbf{t}_1, T_1 \cap T_2) \sin \theta_{\min}(T_1, T_2).$$

Proof. We may reduce the problem to the case where $T_1 \cap T_2 = \{0\}$. Indeed, let $\tilde{T}_1 = T_1 \cap T_2^\perp$, $\tilde{T}_2 = T_1^\perp \cap T_2$ and $\tilde{\mathbf{t}}_1 = \mathbf{t}_1 - P_{T_1 \cap T_2}(\mathbf{t}_1)$. Then

$$\|\mathbf{t}_1 - P_{T_2}(\mathbf{t}_1)\| = \|\tilde{\mathbf{t}}_1 - P_{\tilde{T}_2}(\tilde{\mathbf{t}}_1)\|, \quad \|\mathbf{t}_1 - P_{T_1 \cap T_2}(\mathbf{t}_1)\| = \|\tilde{\mathbf{t}}_1\|, \quad \sin \theta_{\min}(T_1, T_2) = \sin \theta_{\min}(\tilde{T}_1, \tilde{T}_2).$$

So assume that $T_1 \cap T_2 = \{0\}$. By ([Afriat, 1957](#), Th. 10.1), the angle formed by \mathbf{t}_1 and $P_{T_2}(\mathbf{t}_1)$ is at least as large as the smallest principal angle between T_1 and T_2 , which is $\theta_{\min}(T_1, T_2)$ since $T_1 \cap T_2 = \{0\}$. From this the result follows immediately. \square

The following result says that a point cannot be close to two compact and smooth surfaces intersecting at a positive angle without being close to their intersection. Note that the constant there cannot be solely characterized by κ , as it also depends on the separation between the surfaces away from their intersection.

Lemma 18. *Suppose $S_1, S_2 \in \mathcal{S}_d(\kappa)$ intersect at a strictly positive angle and that $\text{reach}(S_1 \cap S_2) \geq 1/\kappa$. Then there is a constant C_{18} such that*

$$\text{dist}(\mathbf{x}, S_1 \cap S_2) \leq C_{18} \max \{ \text{dist}(\mathbf{x}, S_1), \text{dist}(\mathbf{x}, S_2) \}, \quad \forall \mathbf{x} \in \mathbb{R}^D. \quad (25)$$

Proof. Assume the result is not true, so there is a sequence $(\mathbf{x}_n) \subset \mathbb{R}^D$ such that $\text{dist}(\mathbf{x}_n, S_1 \cap S_2) > n \max_k \text{dist}(\mathbf{x}_n, S_k)$. Because the surfaces are bounded, we may assume WLOG that the sequence is bounded. Then $\text{dist}(\mathbf{x}_n, S_1 \cap S_2)$ is bounded, which implies $\max_k \text{dist}(\mathbf{x}_n, S_k) = O(1/n)$. This also forces $\text{dist}(\mathbf{x}_n, S_1 \cap S_2) \rightarrow 0$. Indeed, otherwise there is a constant $C > 0$ and a subsequence $(\mathbf{x}_{n'})$ such that $\text{dist}(\mathbf{x}_{n'}, S_1 \cap S_2) \geq C$. Since $(\mathbf{x}_{n'})$ is bounded, there is a subsequence $(\mathbf{x}_{n''})$ that converges, and by the fact that $\max_k \text{dist}(\mathbf{x}_{n''}, S_k) = o(1)$, and by compactness of S_k , the limit is necessarily in $S_1 \cap S_2$, which is a contradiction. So we have $\text{dist}(\mathbf{x}_n, S_1 \cap S_2) = o(1)$, implying $\max_k \text{dist}(\mathbf{x}_n, S_k) = o(1/n)$.

Assume n is large enough that $\text{dist}(\mathbf{x}_n, S_1 \cap S_2) < 1/\kappa$ and let \mathbf{s}_n^k be the projection of \mathbf{x}_n onto S_k , and \mathbf{s}_n^\dagger the projection of \mathbf{x}_n onto $S_1 \cap S_2$. Let $T_k = T_{S_k}(\mathbf{s}_n^k)$ and note that $\theta_{\min}(T_1, T_2) \geq \theta$, where $\theta > 0$ is the minimum intersection angle between S_1 and S_2 defined in (10). Let \mathbf{t}_n^k be the

projection of \mathbf{s}_n^k onto T_k . Assume WLOG that $\|\mathbf{t}_n^1 - \mathbf{s}_n^1\| \geq \|\mathbf{t}_n^2 - \mathbf{s}_n^2\|$. Let \mathbf{t}_n denote the projection of \mathbf{t}_n^1 onto $T_1 \cap T_2$, and then let $\mathbf{s}_n = P_{S_1 \cap S_2}(\mathbf{t}_n)$.

By assumption, we have

$$n \max_k \|\mathbf{x}_n - \mathbf{s}_n^k\| \leq \|\mathbf{x}_n - \mathbf{s}_n^\dagger\| = o(1). \quad (26)$$

We start with the RHS:

$$\|\mathbf{x}_n - \mathbf{s}_n^\dagger\| = \min_{\mathbf{s} \in S_1 \cap S_2} \|\mathbf{x}_n - \mathbf{s}\| \leq \|\mathbf{x}_n - \mathbf{s}_n\|, \quad (27)$$

and first show that $\|\mathbf{x}_n - \mathbf{s}_n\| = o(1)$ too. We use the triangle inequality multiple times in what follows. We have

$$\|\mathbf{x}_n - \mathbf{s}_n\| \leq \|\mathbf{x}_n - \mathbf{s}_n^1\| + \|\mathbf{s}_n^1 - \mathbf{t}_n^1\| + \|\mathbf{t}_n^1 - \mathbf{t}_n\| + \|\mathbf{t}_n - \mathbf{s}_n\|. \quad (28)$$

From (26), $\|\mathbf{x}_n - \mathbf{s}_n^1\| = o(1)$ and $\|\mathbf{x}_n - \mathbf{s}_n^\dagger\| = o(1)$, and so that by (16),

$$\|\mathbf{s}_n^1 - \mathbf{t}_n^1\| \leq \kappa \|\mathbf{s}_n^1 - \mathbf{s}_n^\dagger\|^2 \leq 2\kappa (\|\mathbf{s}_n^1 - \mathbf{x}_n\|^2 + \|\mathbf{x}_n - \mathbf{s}_n^\dagger\|^2) = o(1). \quad (29)$$

We also have

$$\|\mathbf{t}_n^1 - \mathbf{t}_n\| = \min_{\mathbf{t} \in T_1 \cap T_2} \|\mathbf{t}_n^1 - \mathbf{t}\| \leq \|\mathbf{t}_n^1 - \mathbf{s}_n^\dagger\| \leq \|\mathbf{t}_n^1 - \mathbf{s}_n^1\| + \|\mathbf{s}_n^1 - \mathbf{x}_n\| + \|\mathbf{x}_n - \mathbf{s}_n^\dagger\| = o(1), \quad (30)$$

where the first inequality comes from $\mathbf{s}_n^\dagger \in T_1 \cap T_2$. Finally,

$$\|\mathbf{t}_n - \mathbf{s}_n\| = \min_{\mathbf{s} \in S_1 \cap S_2} \|\mathbf{t}_n - \mathbf{s}\| \leq \|\mathbf{t}_n - \mathbf{s}_n^\dagger\| \leq \|\mathbf{t}_n - \mathbf{t}_n^1\| + \|\mathbf{t}_n^1 - \mathbf{s}_n^\dagger\| = o(1),$$

where the first inequality comes from $\mathbf{s}_n^\dagger \in S_1 \cap S_2$.

We now proceed. The last upper bound is rather crude. Indeed, we use (18) for $S = S_1 \cap S_2$ and $\mathbf{s} = \mathbf{s}_n^\dagger$, noting that $T_{S_1 \cap S_2}(\mathbf{s}_n^\dagger) = T_1 \cap T_2$ and $\|\mathbf{t}_n - \mathbf{s}_n^\dagger\| = o(1)$, and get

$$\|\mathbf{t}_n - \mathbf{s}_n\| \leq \kappa \|\mathbf{t}_n - \mathbf{s}_n^\dagger\|^2 \leq \kappa (\|\mathbf{t}_n - \mathbf{s}_n\| + \|\mathbf{s}_n - \mathbf{x}_n\| + \|\mathbf{x}_n - \mathbf{s}_n^\dagger\|)^2.$$

We have $\|\mathbf{x}_n - \mathbf{s}_n^\dagger\| = \|\mathbf{x}_n - P_{S_1 \cap S_2}(\mathbf{x}_n)\| \leq \|\mathbf{x}_n - \mathbf{s}_n\|$ because $\mathbf{s}_n \in T_1 \cap T_2$. This leads to

$$\|\mathbf{t}_n - \mathbf{s}_n\| \leq \kappa (\|\mathbf{t}_n - \mathbf{s}_n\| + 2\|\mathbf{s}_n - \mathbf{x}_n\|)^2 \leq 4\kappa \|\mathbf{x}_n - \mathbf{s}_n\|^2, \quad (31)$$

eventually, since $\|\mathbf{t}_n - \mathbf{s}_n\| = o(1)$.

Combining (28), (29) and (31), we get

$$\|\mathbf{x}_n - \mathbf{s}_n\| \leq \|\mathbf{x}_n - \mathbf{s}_n^1\| + O(\|\mathbf{x}_n - \mathbf{s}_n^1\|^2 + \|\mathbf{x}_n - \mathbf{s}_n\|^2) + \|\mathbf{t}_n^1 - \mathbf{t}_n\| + O(\|\mathbf{x}_n - \mathbf{s}_n\|^2),$$

which leads to

$$\|\mathbf{x}_n - \mathbf{s}_n\| \leq 2\|\mathbf{x}_n - \mathbf{s}_n^1\| + 2\|\mathbf{t}_n^1 - \mathbf{t}_n\|, \quad (32)$$

when n is large enough. Using this bound in (26) combined with (27), we get

$$\|\mathbf{t}_n^1 - \mathbf{t}_n\| \geq \frac{n-2}{2} \max_k \|\mathbf{x}_n - \mathbf{s}_n^k\|.$$

We then have

$$\begin{aligned}
\max_k \|\mathbf{x}_n - \mathbf{s}_n^k\| &\geq \frac{1}{2} \|\mathbf{s}_n^1 - \mathbf{s}_n^2\| \\
&\geq \frac{1}{2} (\|\mathbf{t}_n^1 - \mathbf{t}_n^2\| - \|\mathbf{s}_n^1 - \mathbf{t}_n^1\| - \|\mathbf{s}_n^2 - \mathbf{t}_n^2\|) \\
&\geq \frac{1}{2} \text{dist}(\mathbf{t}_n^1, T_2) - \|\mathbf{s}_n^1 - \mathbf{t}_n^1\|,
\end{aligned}$$

with

$$\|\mathbf{s}_n^1 - \mathbf{t}_n^1\| = O(\|\mathbf{x}_n - \mathbf{s}_n^1\|^2 + \|\mathbf{x}_n - \mathbf{s}_n^\dagger\|^2) = O(\|\mathbf{x}_n - \mathbf{s}_n\|^2) = O(\|\mathbf{t}_n^1 - \mathbf{t}_n\|^2),$$

due (in the same order) to (29), (26)-(27), and (32). Recalling that $\|\mathbf{t}_n^1 - \mathbf{t}_n\| = \text{dist}(\mathbf{t}_n^1, T_1 \cap T_2)$, we conclude that

$$\text{dist}(\mathbf{t}_n^1, T_2) = O(1/n) \text{dist}(\mathbf{t}_n^1, T_1 \cap T_2) + O(1) \text{dist}(\mathbf{t}_n^1, T_1 \cap T_2)^2.$$

However, by Lemma 17, $\text{dist}(\mathbf{t}_n^1, T_2) \geq (\sin \theta) \text{dist}(\mathbf{t}_n^1, T_1 \cap T_2)$, so that dividing by $\text{dist}(\mathbf{t}_n^1, T_2)$ above leads to $1 = O(1/n) + O(1) \text{dist}(\mathbf{t}_n^1, T_2)$, which is in contradiction with the fact that $\text{dist}(\mathbf{t}_n^1, T_2) \leq \|\mathbf{t}_n^1 - \mathbf{t}_n\| = o(1)$, established in (30). \square

6.1.6 Covariances near an intersection

We look at covariance matrices near an intersection. We start with a continuity result.

Lemma 19. *Let T_1 and T_2 be two linear subspaces of same dimension d . For $\mathbf{x} \in T_1$, denote by $\Sigma(\mathbf{x})$ the covariance matrix of the uniform distribution over $B(\mathbf{x}, 1) \cap (T_1 \cup T_2)$. Then, for all $\mathbf{x}, \mathbf{y} \in T_1$,*

$$\|\Sigma(\mathbf{x}) - \Sigma(\mathbf{y})\| \leq \begin{cases} 5d \|\mathbf{x} - \mathbf{y}\|, & \text{if } d \geq 2, \\ \sqrt{6} \|\mathbf{x} - \mathbf{y}\|, & \text{if } d = 1. \end{cases}$$

Proof. Since, by Lemma 11, $\Sigma(\mathbf{x}) = cP_{T_1}$ for all $\mathbf{x} \in T_1$ such that $\text{dist}(\mathbf{x}, T_2) \geq 1$, we may assume that $\text{dist}(\mathbf{x}, T_1) < 1$ and $\text{dist}(\mathbf{y}, T_1) < 1$. Let $d = \dim(T_1) = \dim(T_2)$ and $A_{\mathbf{x}}^j = B(\mathbf{x}, 1) \cap T_j$ for any \mathbf{x} and $j = 1, 2$. By Lemma 12 and then Lemma 5, we have

$$\begin{aligned}
\|\Sigma(\mathbf{x}) - \Sigma(\mathbf{y})\| &= \|\text{Cov}(\lambda_{A_{\mathbf{x}}^1 \cup A_{\mathbf{x}}^2}) - \text{Cov}(\lambda_{A_{\mathbf{y}}^1 \cup A_{\mathbf{y}}^2})\| \\
&\leq \text{TV}(\lambda_{A_{\mathbf{x}}^1 \cup A_{\mathbf{x}}^2}, \lambda_{A_{\mathbf{y}}^1 \cup A_{\mathbf{y}}^2}) \\
&\leq 4 \frac{\text{vol}((A_{\mathbf{x}}^1 \cup A_{\mathbf{x}}^2) \Delta (A_{\mathbf{y}}^1 \cup A_{\mathbf{y}}^2))}{\text{vol}((A_{\mathbf{x}}^1 \cup A_{\mathbf{x}}^2) \cup (A_{\mathbf{y}}^1 \cup A_{\mathbf{y}}^2))} \\
&\leq 4 \frac{\text{vol}(A_{\mathbf{x}}^1 \Delta A_{\mathbf{y}}^1) + \text{vol}(A_{\mathbf{x}}^2 \Delta A_{\mathbf{y}}^2)}{\text{vol}(A_{\mathbf{x}}^1)}.
\end{aligned}$$

Note that $A_{\mathbf{x}}^1$ is the unit-radius ball of T_1 centered at \mathbf{x} , while $A_{\mathbf{x}}^2$ is the ball of T_2 centered at $\mathbf{x}_2 := P_{T_2}(\mathbf{x})$ and of radius $\eta := \sqrt{1 - \|\mathbf{x} - \mathbf{x}_2\|^2}$. Similarly, $A_{\mathbf{y}}^1$ is the unit-radius ball of T_1 centered at \mathbf{y} , while $A_{\mathbf{y}}^2$ is the ball of T_2 centered at $\mathbf{y}_2 := P_{T_2}(\mathbf{y})$ and of radius $\delta := \sqrt{1 - \|\mathbf{y} - \mathbf{y}_2\|^2}$. Therefore, applying Lemma 10, we get

$$\frac{\text{vol}(A_{\mathbf{x}}^1 \Delta A_{\mathbf{y}}^1)}{2 \text{vol}(A_{\mathbf{x}}^1)} \leq 1 - (1 - t)_+^d,$$

and assuming WLOG that $\delta \leq \eta$, and after proper scaling, we get

$$\frac{\text{vol}(A_{\mathbf{x}}^2 \triangle A_{\mathbf{y}}^2)}{2 \text{vol}(A_{\mathbf{x}}^1)} \leq \zeta := \eta^d - (\eta - t_2)_+^d \wedge \delta^d,$$

where $t := \|\mathbf{x} - \mathbf{y}\|$ and $t_2 := \|\mathbf{x}_2 - \mathbf{y}_2\|$ — note that $t_2 \leq t$ by the fact that P_{T_2} is 1-Lipschitz.

We have $1 - (1 - t)_+^d \leq dt$. This is obvious when $t \geq 1$, while when $t \leq 1$ it is obtained using the fact that, for any $0 \leq s < t \leq 1$,

$$t^d - s^d = (t - s)(t^{d-1} + st^{d-2} + \dots + s^{d-2}t + s^{d-1}) \leq dt^{d-1}(t - s) \leq d(t - s). \quad (33)$$

For the second ratio, we consider several cases.

- When $\eta \leq t_2$, then $\zeta = \eta^d \leq \eta \leq t_2 \leq t$.
- When $t_2 < \eta \leq t_2 + \delta$, then $\zeta = \eta^d - (\eta - t_2)^d \leq dt_2 \leq dt$.
- When $\eta \geq t_2 + \delta$ and $d \geq 2$, we have

$$\begin{aligned} \zeta &= \eta^d - \delta^d \leq d\eta(\eta - \delta) \leq d(\eta^2 - \delta^2) \\ &= d(\|\mathbf{y} - \mathbf{y}_2\|^2 - \|\mathbf{x} - \mathbf{x}_2\|^2) \\ &= d(\|\mathbf{y} - \mathbf{y}_2\| + \|\mathbf{x} - \mathbf{x}_2\|)(\|\mathbf{y} - \mathbf{y}_2\| - \|\mathbf{x} - \mathbf{x}_2\|) \\ &\leq 2d(t + t_2) \leq 4dt, \end{aligned}$$

where the triangle inequality was applied in the last inequality, in the form of

$$\|\mathbf{y} - \mathbf{y}_2\| \leq \|\mathbf{y} - \mathbf{x}\| + \|\mathbf{x} - \mathbf{x}_2\| + \|\mathbf{x}_2 - \mathbf{x}\| = \|\mathbf{x} - \mathbf{x}_2\| + t + t_2.$$

- When $\eta \geq t_2 + \delta$ and $d = 1$, we have

$$\zeta = \eta - \delta \leq \sqrt{\|\mathbf{y} - \mathbf{y}_2\| - \|\mathbf{x} - \mathbf{x}_2\|} \leq \sqrt{t + t_2} \leq \sqrt{2t},$$

using the same triangle inequality and the fact that, for any $0 \leq s < t \leq 1$,

$$0 \leq \sqrt{1 - s} - \sqrt{1 - t} = \frac{t - s}{\sqrt{1 - s} + \sqrt{1 - t}} \leq \frac{t - s}{\sqrt{1 - t + t - s}} \leq \frac{t - s}{\sqrt{t - s}} = \sqrt{t - s}.$$

When $d \geq 2$, we can therefore bound $\|\Sigma(\mathbf{x}) - \Sigma(\mathbf{y})\|$ by $dt + 4dt = 5dt$, and when $d = 1$, we bound that by $t + \sqrt{2t} \leq \sqrt{6t}$. \square

The following is in some sense a converse to Lemma 19, in that we lower-bound the distance between covariance matrices near an intersection of linear subspaces. Note that the covariance matrix does not change when moving parallel to the intersection; however, it does when moving perpendicular to the intersection.

Lemma 20. *Let T_1 and T_2 be two linear subspaces of same dimension with $\theta_{\min}(T_1, T_2) \geq \theta_0 > 0$. Fix a unit norm vector $\mathbf{v} \in T_1 \cap (T_1 \cap T_2)^\perp$. With $\Sigma(h\mathbf{v})$ denoting the covariance of the uniform distribution over $B(h\mathbf{v}, 1) \cap (T_1 \cup T_2)$, we have*

$$\inf_h \sup_\ell \|\Sigma(h\mathbf{v}) - \Sigma(\ell\mathbf{v})\| \geq 1/C_{20},$$

where the infimum is over $0 < h < 1/\sin \theta_0$ and the supremum over $\max(0, h - 1/2) \leq \ell \leq \min(1/\sin \theta_0, h + 1/2)$, and $C_{20} > 0$ depends only on d and θ_0 .

Proof. If the statement of the lemma is not true, there are subspaces T_1 and T_2 of same dimension d , a unit length vector $\mathbf{v} \in T_1 \cap (T_1 \cap T_2)^\perp$ and $0 \leq h \leq 1/\sin \theta_0$, such that

$$\Sigma(\ell\mathbf{v}) = \Sigma(h\mathbf{v}) \text{ for all } \max(0, h - 1/2) \leq \ell \leq \min(1/\sin \theta_0, h + 1/2). \quad (34)$$

By projecting onto $(T_1 \cap T_2)^\perp$, we may assume that $T_1 \cap T_2 = 0$ without loss of generality. Let $\theta = \angle(\mathbf{v}, T_2)$ and note that $\theta \geq \theta_0$ since $T_1 \cap T_2 = 0$. Define $\mathbf{u} = (\mathbf{v} - P_{T_2}\mathbf{v})/\sin \theta$ and also $\mathbf{w} = P_{T_2}\mathbf{v}/\cos \theta$ when $\theta < \pi/2$, and $\mathbf{w} \in T_2$ is any vector perpendicular to \mathbf{v} when $\theta = \pi/2$. $B(h\mathbf{v}, 1) \cap T_1$ is the d -dimensional ball of T_1 of radius 1 and center $h\mathbf{v}$, while — using Pythagoras theorem — $B(h\mathbf{v}, 1) \cap T_2$ is the d -dimensional ball of T_2 of radius $t := (1 - (h \sin \theta)^2)^{1/2}$ and center $(h \cos \theta)\mathbf{w}$. Let X be drawn from the uniform distribution over $B(h\mathbf{v}, 1) \cap (T_1 \cup T_2)$, while X_0 and X'_0 are independently drawn from the uniform distributions over the unit balls of T_1 and T_2 , respectively. By Lemma 11, $\text{Cov}(X_0) = cP_{T_1}$ and $\text{Cov}(X'_0) = cP_{T_2}$ where $c := 1/(d + 2)$. Also, let ξ be Bernoulli with parameter α , where

$$\alpha := \frac{\text{vol}(B(h\mathbf{v}, 1) \cap T_1)}{\text{vol}(B(h\mathbf{v}, 1) \cap (T_1 \cup T_2))} = \frac{\text{vol}(B(h\mathbf{v}, 1) \cap T_1)}{\text{vol}(B(h\mathbf{v}, 1) \cap T_1) + \text{vol}(B((h \cos \theta)\mathbf{w}, t) \cap T_2)} = \frac{1}{1 + t^d}.$$

We have

$$X \sim \xi(h\mathbf{v} + X_0) + (1 - \xi)((h \cos \theta)\mathbf{w} + tX'_0).$$

A straightforward calculation, or an application of the law of total covariance, leads to

$$\text{Cov}(X) = \mathbb{E}(\xi) \text{Cov}(X_0) + \mathbb{E}(1 - \xi)t^2 \text{Cov}(X'_0) + \text{Var}(\xi)h^2(\mathbf{v} - (\cos \theta)\mathbf{w})(\mathbf{v} - (\cos \theta)\mathbf{w})^\top, \quad (35)$$

which simplifies to

$$\Sigma(h\mathbf{v}) = c\alpha P_{T_1} + c(1 - \alpha)t^2 P_{T_2} + \alpha(1 - \alpha)(1 - t^2)\mathbf{u}\mathbf{u}^\top,$$

using the fact that $\mathbf{v} - (\cos \theta)\mathbf{w} = (\sin \theta)\mathbf{u}$ and the definition of t . Let $\theta_1 = \theta_{\max}(T_1, T_2)$ and let $\mathbf{v}_1 \in T_1$ be of unit length and such that $\angle(\mathbf{v}_1, T_2) = \theta_1$. Then for any $0 \leq h, \ell \leq 1/\sin \theta_0$, we have

$$\|\Sigma(h\mathbf{v}) - \Sigma(\ell\mathbf{v})\| \geq |\mathbf{v}_1^\top \Sigma(h\mathbf{v})\mathbf{v}_1 - \mathbf{v}_1^\top \Sigma(\ell\mathbf{v})\mathbf{v}_1| = |f(t_h) - f(t_\ell)|, \quad (36)$$

where $t_h := (1 - (h \sin \theta)^2)^{1/2}$ and

$$f(t) = \frac{c}{1 + t^d} + \frac{ct^{d+2}(\cos \theta_1)^2}{1 + t^d} + \frac{t^d(1 - t^2)(\mathbf{u}^\top \mathbf{v}_1)^2}{(1 + t^d)^2}.$$

It is easy to see that the interval

$$I_h = \{t_\ell : (h - 1/2)_+ \leq \ell \leq (1/\sin \theta_0) \wedge (h + 1/2)\}$$

is non empty. Because of (34) and (36), $f(t)$ is constant over $t \in I_h$, but this is not possible since f is a rational function not equal to a constant and therefore cannot be constant over an interval of positive length. \square

We now look at the eigenvalues of the covariance matrix.

Lemma 21. *Let T_1 and T_2 be two linear subspaces of same dimension d . For $\mathbf{x} \in T_1$, denote by $\Sigma(\mathbf{x})$ the covariance matrix of the uniform distribution over $B(\mathbf{x}, 1) \cap (T_1 \cup T_2)$. Then, for all $\mathbf{x} \in T_1$,*

$$c(1 - (1 - \delta^2(\mathbf{x}))_+^{d/2}) \leq \beta_d(\Sigma(\mathbf{x})), \quad \beta_1(\Sigma(\mathbf{x})) \leq c + \delta(\mathbf{x})(1 - \delta^2(\mathbf{x}))_+^{d/2}, \quad (37)$$

$$\frac{c}{8}(1 - \cos \theta_{\max}(T_1, T_2))^2(1 - \delta^2(\mathbf{x}))_+^{d/2+1} \leq \beta_{d+1}(\Sigma(\mathbf{x})) \leq (c + \delta^2(\mathbf{x}))(1 - \delta^2(\mathbf{x}))_+^{d/2}, \quad (38)$$

where $c := 1/(d + 2)$ and $\delta(\mathbf{x}) := \text{dist}(\mathbf{x}, T_2)$.

Proof. As in (35), we have

$$\Sigma(\mathbf{x}) = \alpha c P_{T_1} + (1 - \alpha) c t^2 P_{T_2} + \alpha(1 - \alpha)(\mathbf{x} - \mathbf{x}_2)(\mathbf{x} - \mathbf{x}_2)^\top, \quad (39)$$

where $\mathbf{x}_2 := P_{T_2}(\mathbf{x})$ and $\alpha := (1 + t^d)^{-1}$ with $t := (1 - \delta^2(\mathbf{x}))_+^{1/2}$. Because all the matrices in this display are positive semidefinite, we have

$$\beta_d(\Sigma(\mathbf{x})) \geq \alpha c \|P_{T_1}\| = \alpha c,$$

with $\alpha \geq 1 - t^d$. And because of the triangle inequality, we have

$$\beta_1(\Sigma(\mathbf{x})) \leq \alpha c \|P_{T_1}\| + (1 - \alpha) c t^2 \|P_{T_2}\| + \alpha(1 - \alpha) \|\mathbf{x} - \mathbf{x}_2\|^2 \leq c + \alpha(1 - \alpha) \delta^2(\mathbf{x}),$$

with $\alpha(1 - \alpha) \leq t^d$. Hence, (37) is proved.

For the upper bound in (38), by Weyl's inequality (Stewart and Sun, 1990, Cor. IV.4.9) and the fact that $\beta_{d+1}(P_{T_1}) = 0$, and then the triangle inequality, we get

$$\begin{aligned} \beta_{d+1}(\Sigma(\mathbf{x})) &\leq \|\Sigma(\mathbf{x}) - \alpha c P_{T_1}\| \\ &\leq c(1 - \alpha) t^2 \|P_{T_2}\| + \alpha(1 - \alpha) \delta^2(\mathbf{x}) \\ &\leq (1 - \alpha)(c + \delta^2(\mathbf{x})), \end{aligned}$$

and we then use the fact that $1 - \alpha \leq t^d$. For the lower bound, let $\theta_1 \geq \theta_2 \geq \dots \geq \theta_d$ denote the principal angles between T_1 and T_2 . By definition of principal angles, there are orthonormal bases for T_1 and T_2 , denoted $\mathbf{v}_1, \dots, \mathbf{v}_d$ and $\mathbf{w}_1, \dots, \mathbf{w}_d$, such that $\mathbf{v}_j^\top \mathbf{w}_k = \mathbb{I}_{j=k} \cdot \cos \theta_j$. Take $\mathbf{u} \in \text{span}(\mathbf{v}_1, \dots, \mathbf{v}_d, \mathbf{w}_1)$, that is, of the form $\mathbf{u} = a\mathbf{v}_1 + \mathbf{v} + b\mathbf{w}_1$, with $\mathbf{v} \in \text{span}(\mathbf{v}_2, \dots, \mathbf{v}_d)$. Since $P_{T_1} = \mathbf{v}_1\mathbf{v}_1^\top + \dots + \mathbf{v}_d\mathbf{v}_d^\top$ and $P_{T_2} = \mathbf{w}_1\mathbf{w}_1^\top + \dots + \mathbf{w}_d\mathbf{w}_d^\top$, we have

$$\begin{aligned} \frac{1}{c} \mathbf{u}^\top \Sigma(\mathbf{x}) \mathbf{u} &\geq \alpha(a^2 + \|\mathbf{v}\|^2 + 2ab \cos \theta_1 + b^2 \cos^2 \theta_1) + (1 - \alpha)t^2(b^2 + 2ab \cos \theta_1 + a^2 \cos^2 \theta_1) \\ &= \alpha(a + b \cos \theta_1)^2 + (1 - \alpha)t^2(a \cos \theta_1 + b)^2 + \alpha(1 - a^2 - b^2), \end{aligned}$$

assuming $\|\mathbf{u}\|^2 = a^2 + \|\mathbf{v}\|^2 + b^2 = 1$. If $|a| \vee |b| \leq 1/2$, then the RHS $\geq \alpha/2 \geq 1/4$. Otherwise, the RHS $\geq (1 - \alpha)t^2(1 - \cos \theta_1)^2/4$, using the fact that $\alpha \geq 1 - \alpha \geq (1 - \alpha)t^2$. Hence, by the Courant-Fischer theorem (Stewart and Sun, 1990, Cor. IV.4.7), we have

$$\beta_{d+1}(\Sigma(\mathbf{x})) \geq \frac{c}{4}(1 - \alpha)t^2(1 - \cos \theta_1)^2,$$

with $1 - \alpha \geq t^d/2$. This proves (38). \square

Below is a technical result on the covariance matrix of the uniform distribution on the intersection of a ball and the union of two smooth surfaces, near where the surfaces intersect. It generalizes Lemma 13.

Lemma 22. *Let $S_1, S_2 \in \mathcal{S}_d(\kappa)$ intersecting at a positive angle, with $\text{reach}(S_1 \cap S_2) \geq 1/\kappa$. Then there is a constant $C_{22} \geq 3$ such that the following holds. Fix $r < 1/C_{22}$, and for $\mathbf{s} \in S_1$ with $\text{dist}(\mathbf{s}, S_2) \leq r$, let $\mathbf{C}(\mathbf{s})$ and $\Sigma(\mathbf{s})$ denote the covariance matrices of the uniform distributions over $B(\mathbf{s}, r) \cap (S_1 \cup S_2)$ and $B(\mathbf{s}, r) \cap (T_1 \cup T_2)$, where $T_1 := T_{S_1}(\mathbf{s})$ and $T_2 := T_{S_2}(P_{S_2}(\mathbf{s}))$. Then*

$$\|\mathbf{C}(\mathbf{s}) - \Sigma(\mathbf{s})\| \leq C_{22} r^3. \quad (40)$$

Proof. Below C denotes a positive constant depending only on S_1 and S_2 that increases with each appearance. We note that it is enough to prove the result when r is small enough. Take $\mathbf{s} \in S_1$ such that $\delta := \text{dist}(\mathbf{s}, S_2) \leq r$ and let $\mathbf{s}_2 = P_{S_2}(\mathbf{s})$ — note that $\|\mathbf{s} - \mathbf{s}_2\| = \delta$. Let B_r be short for $B(\mathbf{s}, r)$ and define $A_k = B_r \cap S_k$, $\boldsymbol{\mu}_k = \mathbb{E}(\lambda_{A_k})$ and $\mathbf{D}_k = \text{Cov}(\lambda_{A_k})$, for $k = 1, 2$. As in (35), we have

$$\mathbf{C}(\mathbf{s}) = \alpha \mathbf{D}_1 + (1 - \alpha) \mathbf{D}_2 + \alpha(1 - \alpha)(\boldsymbol{\mu}_1 - \boldsymbol{\mu}_2)(\boldsymbol{\mu}_1 - \boldsymbol{\mu}_2)^\top,$$

where

$$\alpha := \frac{\text{vol}(A_1)}{\text{vol}(A_1) + \text{vol}(A_2)}.$$

Let $T_1 = T_{S_1}(\mathbf{s})$ and $T_2 = T_{S_2}(\mathbf{s}_2)$, and define $A'_k = B_r \cap T_k$, so that $B_r \cap (T_1 \cup T_2) = A'_1 \cup A'_2$. Note that $\mathbb{E}(\lambda_{A'_1}) = \mathbf{s}$ and $\mathbb{E}(\lambda_{A'_2}) = \mathbf{s}_2$, and by Lemma 11, $\mathbf{D}'_1 := \text{Cov}(\lambda_{A'_1}) = cr^2 P_{T_1}$ and $\mathbf{D}'_2 := \text{Cov}(\lambda_{A'_2}) = c(r^2 - \delta^2) P_{T_2}$, where $c := 1/(d + 2)$. As in (39), we have

$$\boldsymbol{\Sigma}(\mathbf{s}) = \alpha' \mathbf{D}'_1 + (1 - \alpha') \mathbf{D}'_2 + \alpha'(1 - \alpha')(\mathbf{s} - \mathbf{s}_2)(\mathbf{s} - \mathbf{s}_2)^\top,$$

where

$$\alpha' := \frac{\text{vol}(A'_1)}{\text{vol}(A'_1) + \text{vol}(A'_2)}.$$

Since $|\alpha'(1 - \alpha') - \alpha(1 - \alpha)| \leq |\alpha' - \alpha|$, we have

$$\begin{aligned} \|\mathbf{C}(\mathbf{s}) - \boldsymbol{\Sigma}(\mathbf{s})\| &\leq |\alpha' - \alpha|(\|\mathbf{D}'_1\| + \|\mathbf{D}'_2\| + \|\mathbf{s} - \mathbf{s}_2\|^2) \\ &\quad + \alpha\|\mathbf{D}_1 - \mathbf{D}'_1\| + (1 - \alpha)\|\mathbf{D}_2 - \mathbf{D}'_2\| + \alpha(1 - \alpha)4r(\|\boldsymbol{\mu}_1 - \mathbf{s}\| + \|\boldsymbol{\mu}_2 - \mathbf{s}_2\|) \\ &\leq (2c + 1)r^2|\alpha' - \alpha| \\ &\quad + \|\mathbf{D}_1 - \mathbf{D}'_1\| \vee \|\mathbf{D}_2 - \mathbf{D}'_2\| + 2r(\|\boldsymbol{\mu}_1 - \mathbf{s}\| \vee \|\boldsymbol{\mu}_2 - \mathbf{s}_2\|), \end{aligned}$$

using the triangle inequality multiple times, and in the first inequality we used the fact that

$$\|\mathbf{v}\mathbf{v}^\top - \mathbf{w}\mathbf{w}^\top\| \leq \|(\mathbf{v} - \mathbf{w})\mathbf{v}^\top\| + \|\mathbf{w}(\mathbf{v} - \mathbf{w})^\top\| \leq (\|\mathbf{v}\| + \|\mathbf{w}\|)\|\mathbf{v} - \mathbf{w}\|,$$

for any two vectors $\mathbf{v}, \mathbf{w} \in \mathbb{R}^D$. Assuming that $\kappa r \leq 1/C_{13}$, by Lemma 13, we have $\|\boldsymbol{\mu}_1 - \mathbf{s}\| \vee \|\boldsymbol{\mu}_2 - \mathbf{s}_2\| \leq C_{13}\kappa r^2$ and $\|\mathbf{D}_1 - \mathbf{D}'_1\| \vee \|\mathbf{D}_2 - \mathbf{D}'_2\| \leq C_{13}\kappa r^3$. Assuming that $\kappa r \leq 1/3$, $P_{T_k}^{-1}$ is well-defined and $(1 + \kappa r)$ -Lipschitz on $S_k \cap B_r$. And being an orthogonal projection, P_{T_k} is 1-Lipschitz. Hence, applying Lemma 4, we have

$$1 \leq \frac{\text{vol}(A_k)}{\text{vol}(P_{T_k}(A_k))} \leq 1 + \kappa r, \quad k = 1, 2.$$

Then by Lemma 7,

$$1 - C_7\kappa r \leq \frac{\text{vol}(P_{T_k}(A_k))}{\text{vol}(A'_k)} \leq 1 + C_7\kappa r, \quad k = 1, 2.$$

So we get

$$1 - Cr \leq \frac{\text{vol}(A_k)}{\text{vol}(A'_k)} \leq 1 + Cr, \quad k = 1, 2.$$

Since for all $a, b, a', b' > 0$ we have

$$\begin{aligned} \left| \frac{a}{a+b} - \frac{a'}{a'+b'} \right| &\leq \frac{|a - a'| \vee |b - b'|}{(a+b) \vee (a'+b')} \\ &\leq |1 - a/a'| \vee |1 - b/b'|, \end{aligned} \tag{41}$$

we get

$$|\alpha - \alpha'| \leq Cr.$$

Hence,

$$\|\mathbf{C}(\mathbf{s}) - \boldsymbol{\Sigma}(\mathbf{s})\| \leq Cr^3,$$

so we are done with the proof. \square

6.2 Performance guarantees for Algorithm 2

We deal with the case where there is no noise, that is, $\tau = 0$ in (11), so that the data points are $\mathbf{s}_1, \dots, \mathbf{s}_N$, sampled exactly on $S_1 \cup S_2$ according to the uniform distribution. We explain how things change when there is noise, meaning $\tau > 0$, in Section 6.4.

Let $\Xi_i = \{j \neq i : \mathbf{s}_j \in N_r(\mathbf{s}_i)\}$, with (random) cardinality $N_i = |\Xi_i|$. When there is no noise, \mathbf{C}_i is the sample covariance of $\{\mathbf{s}_j : j \in \Xi_i\}$. For $i \in [n]$, let $K_i = 1$ if $\mathbf{s}_i \in S_1$ and $= 2$ otherwise, and let $T_i = T_{S_{K_i}}(\mathbf{s}_i)$, which is the tangent subspace associated with data point \mathbf{s}_i . Given N_i , $\{\mathbf{s}_j : j \in \Xi_i\}$ are uniformly distributed on $S_{K_i} \cap B(\mathbf{s}_i, r)$, and applying Lemma 14 with rescaling, we get that for any $t > 0$

$$\mathbb{P}(\|\mathbf{C}_i - \mathbb{E} \mathbf{C}_i\| > r^2 t \mid N_i) \leq 4d \exp\left(-\frac{N_i t}{C_{14}} \min\left(t, \frac{N_i}{d}\right)\right),$$

for an absolute constant $C_{14} \geq 1$. We may assume that $r < 1/(C_9 \kappa)$ and let $n_\star := nr^d/C_9$. We assume throughout that r is large enough that $n_\star \geq d$, for otherwise the result is void since the probability lower bound stated in Theorem 1 is negative. Using Lemma 9, for any $t < 1$,

$$\begin{aligned} \mathbb{P}(\|\mathbf{C}_i - \mathbb{E} \mathbf{C}_i\| > r^2 t) &\leq \mathbb{P}(\|\mathbf{C}_i - \mathbb{E} \mathbf{C}_i\| > r^2 t \mid N_i \geq n_\star) + \mathbb{P}(N_i < n_\star) \\ &\leq 4d \exp(-n_\star t^2/C_{14}) + C_9 n \exp(-n_\star) \\ &\leq (4d + C_9)n \exp(-n_\star t^2/C_{14}). \end{aligned}$$

Define $\boldsymbol{\Sigma}_i$ as the covariance of the uniform distribution on $T_i \cap B(\mathbf{s}_i, r)$. Let

$$I_\star = \{i : K_j = K_i, \forall j \in \Xi_i\},$$

or equivalently,

$$I_\star^c = \{i : \exists j \text{ s.t. } K_j \neq K_i \text{ and } \|\mathbf{s}_j - \mathbf{s}_i\| \leq r\}.$$

By definition, I_\star indexes the points whose neighborhoods do not contain points from the other cluster. Applying Lemma 13, this leads to

$$\|\mathbb{E} \mathbf{C}_i - \boldsymbol{\Sigma}_i\| \leq C_{13} \kappa r^3, \quad \forall i \in I_\star. \quad (42)$$

Define the events

$$\Omega_1 = \bigcup_{k=1}^2 \{\forall \mathbf{s} \in S_k : \#\{i : K_i = k \text{ and } \mathbf{s}_i \in B(\mathbf{s}, r/C_\Omega)\} > n_\star\},$$

where $C_\Omega := 100d^2 C_{20}^2$, and

$$\Omega_2 = \{\|\mathbf{C}_i - \mathbb{E} \mathbf{C}_i\| \leq r^2 t, \text{ for all } i \in [n]\},$$

and their intersection $\Omega = \Omega_1 \cap \Omega_2$, where $t < 1$ will be determined later. Note that, under Ω_1 , $N_i \geq n_\star$. Applying the union bound,

$$\begin{aligned} \mathbb{P}(\Omega^c) &\leq \mathbb{P}(\Omega_1^c) + \mathbb{P}(\Omega_2^c) \\ &\leq C_9 n \exp(-n_\star) + n(4d + C_9) \exp(-n_\star t^2 / C_{14}) \\ &\leq p_\Omega := (4d + 2C_9)n \exp(-n_\star t^2 / C_{14}). \end{aligned}$$

Assuming that Ω holds, by the triangle inequality, (54) and (42), we have

$$\|\mathbf{C}_i - \boldsymbol{\Sigma}_i\| \leq \|\mathbf{C}_i - \mathbb{E} \mathbf{C}_i\| + \|\mathbb{E} \mathbf{C}_i - \boldsymbol{\Sigma}_i\| \leq \zeta r^2, \quad \forall i \in I_\star, \quad (43)$$

where

$$\zeta := t + C_{13} \kappa r. \quad (44)$$

The inequality (43) leads, via the triangle inequality, to the decisive bound

$$\|\mathbf{C}_i - \mathbf{C}_j\| \leq \|\boldsymbol{\Sigma}_i - \boldsymbol{\Sigma}_j\| + 2\zeta r^2, \quad \forall i, j \in I_\star. \quad (45)$$

Take $i, j \in I_\star$ such that $K_i = K_j$ and $\|\mathbf{s}_i - \mathbf{s}_j\| \leq \varepsilon$. Then by Lemma 11 and Lemma 15, property (20) and the fact that $\sin(2\theta) \leq 2 \sin \theta$ for all θ , and the triangle inequality, we have

$$\frac{1}{cr^2} \|\boldsymbol{\Sigma}_i - \boldsymbol{\Sigma}_j\| = \sin \theta_{\max}(T_i, T_j) \leq 2\kappa \|\mathbf{s}_i - \mathbf{s}_j\| \leq 2\kappa \varepsilon, \quad (46)$$

where $c := 1/(d+2)$. This implies that

$$\frac{1}{r^2} \|\mathbf{C}_i - \mathbf{C}_j\| \leq 2c\kappa \varepsilon + 2\zeta. \quad (47)$$

Therefore, if $\eta > 2c\kappa \varepsilon + 2\zeta$, then any pair of points indexed by $i, j \in I_\star$ from the same cluster and within distance ε are direct neighbors in the graph built by Algorithm 2.

Take $i, j \in I_\star$ such that $K_i \neq K_j$ and $\|\mathbf{s}_i - \mathbf{s}_j\| \leq \varepsilon$. By Lemma 18,

$$\max [\text{dist}(\mathbf{s}_i, S_1 \cap S_2), \text{dist}(\mathbf{s}_j, S_1 \cap S_2)] \leq C_{18} \|\mathbf{s}_i - \mathbf{s}_j\|.$$

Let \mathbf{z} be the mid-point of \mathbf{s}_i and \mathbf{s}_j . By convexity and the display above,

$$\text{dist}(\mathbf{z}, S_1 \cap S_2) \leq \frac{1}{2} \text{dist}(\mathbf{s}_i, S_1 \cap S_2) + \frac{1}{2} \text{dist}(\mathbf{s}_j, S_1 \cap S_2) \leq C_{18} \varepsilon.$$

Assuming $C_{18} \varepsilon < 1/\kappa$, let $\mathbf{s} = P_{S_1 \cap S_2}(\mathbf{z})$. Then, by the triangle inequality again,

$$\max [\|\mathbf{s} - \mathbf{s}_i\|, \|\mathbf{s} - \mathbf{s}_j\|] \leq \text{dist}(\mathbf{z}, S_1 \cap S_2) + \frac{1}{2} \|\mathbf{s}_i - \mathbf{s}_j\| \leq C_{18} \varepsilon + \frac{1}{2} \varepsilon \leq (C_{18} + 1) \varepsilon.$$

Let T'_i denote the tangent subspace of S_{K_i} at \mathbf{s} and let $\boldsymbol{\Sigma}'_i$ be the covariance of the uniform distribution over $T'_i \cap B(\mathbf{s}, r)$. Define T'_j and $\boldsymbol{\Sigma}'_j$ similarly. Then, as in (46) we have

$$\frac{1}{cr^2} \|\boldsymbol{\Sigma}_i - \boldsymbol{\Sigma}'_i\| \leq \kappa \|\mathbf{s}_i - \mathbf{s}\| \leq \kappa (C_{18} + 1) \varepsilon,$$

and similarly,

$$\frac{1}{cr^2} \|\boldsymbol{\Sigma}_j - \boldsymbol{\Sigma}'_j\| \leq \kappa (C_{18} + 1) \varepsilon.$$

Moreover, by Lemma 11 and Lemma 15,

$$\frac{1}{cr^2} \|\boldsymbol{\Sigma}'_i - \boldsymbol{\Sigma}'_j\| = \sin \theta_{\max}(T'_i, T'_j) \geq \sin \theta_S,$$

where θ_S is short for $\theta(S_1, S_2)$. Hence, by the triangle inequality,

$$\frac{1}{cr^2} \|\boldsymbol{\Sigma}_i - \boldsymbol{\Sigma}_j\| \geq \sin \theta_S - 2\kappa(C_{18} + 1)\varepsilon, \quad (48)$$

and then

$$\frac{1}{r^2} \|\mathbf{C}_i - \mathbf{C}_j\| \geq c \sin \theta_S - 2c\kappa(C_{18} + 1)\varepsilon - 2\zeta. \quad (49)$$

Therefore, if $\eta < c \sin \theta_S - 2c\kappa(C_{18} + 1)\varepsilon - 2\zeta$, then any pair of points indexed by $i, j \in I_\star$ from different clusters are *not* direct neighbors in the graph built by Algorithm 2.

In summary, we would like to choose η such that

$$2c\kappa\varepsilon + 2\zeta < \eta < c \sin \theta_S - 2c\kappa(C_{18} + 1)\varepsilon - 2\zeta.$$

This holds when

$$2c\kappa\varepsilon + 2\zeta < \eta < \frac{c \sin \theta_S}{C_{18} + 2},$$

which is true when

$$\varepsilon < \frac{(d+2)\eta}{6\kappa}, \quad t \leq \frac{\eta}{6}, \quad r \leq \frac{\eta}{6C_{13}\kappa}, \quad \eta < \frac{\sin \theta_S}{(C_{18} + 2)(d+2)}, \quad (50)$$

using the definition of ζ in (44) and that of $c = 1/(d+2)$. We choose $t = \eta/6$ and get that $\mathbb{P}(\Omega^c) \leq Cn \exp(-nr^d \eta^2/C)$, where C depends only on d and C_9 .

6.2.1 The different clusters are in different connected components

We show that Step 3 in Algorithm 2 eliminates all points $i \notin I_\star$, implying by our choice of parameters in (50) that after that step the two clusters are not connected to each other in the graph. Hence, take $i \notin I_\star$ with $K_i = 1$ (say), so that $\text{dist}(\mathbf{s}_i, S_2) \leq r$. By Lemma 18, we have $\text{dist}(\mathbf{s}_i, S_1 \cap S_2) \leq C_{18}r < 1/\kappa$. Assuming that $(C_{18} + 1)r < 1/\kappa$, let $\mathbf{s}^0 = P_{S_1 \cap S_2}(\mathbf{s}_i)$ and define $T_k^0 = T_{S_k}(\mathbf{s}^0)$

Below, $C > 0$ is a constant whose value increases with each appearance. By Lemma 22 (and the notation there), for $\mathbf{s} \in S_1$ such that $\text{dist}(\mathbf{s}, S_2) \leq (C_{18} + 1)r$,

$$\|\mathbf{C}(\mathbf{s}) - \boldsymbol{\Sigma}(\mathbf{s})\| \leq Cr^3.$$

We now derive another approximation that involves $\boldsymbol{\Sigma}^0(\mathbf{s})$, the covariance matrix of the uniform distribution on $B(P_{T_1^0}(\mathbf{s}), r) \cap (T_1^0 \cup T_2^0)$. For that, we continue with the notation used in the proof of Lemma 22 until (52) below. Define $\mathbf{t}_1 = P_{T_1^0}(\mathbf{s})$ and $\mathbf{t}_2 = P_{T_2^0}(\mathbf{t}_1)$. Let $\delta_0 = \|\mathbf{t}_1 - \mathbf{t}_2\|$, $\delta_1 = \|\mathbf{s} - \mathbf{t}_1\|$, $\delta_2 = \|\mathbf{s}_2 - \mathbf{t}_2\|$ and $A_k^0 = T_k^0 \cap B(\mathbf{t}_1, r)$. By Lemma 1, we have $\delta_1 \leq Cr^2$ and $\delta_2 \leq Cr^2$, because $\|\mathbf{s} - \mathbf{s}^0\| \leq Cr$ by Lemma 18, and

$$\|\mathbf{s}_2 - \mathbf{s}^0\| \leq \|\mathbf{s}_2 - \mathbf{s}\| + \|\mathbf{s} - \mathbf{s}^0\|.$$

Hence, $|\delta_0 - \delta| \leq \delta_1 + \delta_2 \leq Cr^2$. We assume that r is small enough that $Cr^2 < r$, so that $A_1^0 \neq \emptyset$. Note that $\mathbb{E}(\lambda_{A_k^0}) = \mathbf{t}_k$ and $\mathbf{D}_1^0 := \text{Cov}(\lambda_{A_1^0}) = cr^2 P_{T_1^0}$, while $\mathbf{D}_2^0 := \text{Cov}(\lambda_{A_2^0}) = c(r^2 - \delta_0^2) P_{T_2^0}$ when $\delta_0 \leq r$; otherwise $A_2^0 = \emptyset$. As in (39), we have

$$\boldsymbol{\Sigma}^0(\mathbf{s}) = \alpha^0 \mathbf{D}_1^0 + (1 - \alpha^0) \mathbf{D}_2^0 + \alpha^0(1 - \alpha^0)(\mathbf{t}_1 - \mathbf{t}_2)(\mathbf{t}_1 - \mathbf{t}_2)^\top, \quad (51)$$

where

$$\alpha^0 := \frac{\text{vol}(A_1^0)}{\text{vol}(A_1^0) + \text{vol}(A_2^0)}.$$

This identity remains valid even when $A_2^0 = \emptyset$. As in the proof of Lemma 22, we have

$$\|\Sigma(\mathbf{s}) - \Sigma^0(\mathbf{s})\| \leq (2c+1)r^2|\alpha' - \alpha^0| + \|\mathbf{D}'_1 - \mathbf{D}_1^0\| \vee \|\mathbf{D}'_2 - \mathbf{D}_2^0\| + 2r(\|\mathbf{t}_1 - \mathbf{s}\| \vee \|\mathbf{t}_2 - \mathbf{s}_2\|).$$

By the triangle inequality and the fact that $\|P_T\| \leq 1$ for any subspace T ,

$$\|\mathbf{D}'_1 - \mathbf{D}_1^0\| \leq cr^2\|P_{T_1} - P_{T_1^0}\|,$$

and

$$\|\mathbf{D}'_2 - \mathbf{D}_2^0\| \leq cr^2\|P_{T_2} - P_{T_2^0}\| + c|\delta^2 - \delta_0^2|.$$

By Lemma 2 and Lemma 15, we have

$$\|P_{T_1} - P_{T_1^0}\| \leq \kappa\|\mathbf{s} - \mathbf{s}^0\| \leq Cr, \quad \|P_{T_2} - P_{T_2^0}\| \leq \kappa\|\mathbf{s}_2 - \mathbf{s}_2^0\| \leq Cr.$$

And since $|\delta^2 - \delta_0^2| \leq 2r|\delta - \delta_0| \leq Cr^3$, we have $\|\mathbf{D}'_k - \mathbf{D}_k^0\| \leq Cr^3$ for $k = 1, 2$. Let ω_d denote the volume of the d -dimensional unit ball. Then

$$\text{vol}(A'_1) = \omega_d r^d, \quad \text{vol}(A'_2) = \omega_d(r^2 - \delta^2)^{d/2}, \quad \text{vol}(A_1^0) = \omega_d r^2, \quad \text{vol}(A_2^0) = \omega_d(r^2 - \delta_0^2)_+^{d/2},$$

so that

$$\begin{aligned} |\alpha' - \alpha^0| &= \left| \frac{1}{1 + (1 - \delta/r)^{d/2}} - \frac{1}{1 + (1 - \delta_0/r)_+^{d/2}} \right| \\ &\leq |(1 - \delta/r)^{d/2} - (1 - \delta_0/r)_+^{d/2}|. \end{aligned}$$

Proceeding exactly as when we bounded ζ in the proof of Lemma 19, we get

$$|\alpha' - \alpha^0| \leq d\sqrt{|\delta - \delta_0|/r} \leq C\sqrt{r}.$$

Hence, we proved that

$$\|\Sigma(\mathbf{s}) - \Sigma^0(\mathbf{s})\| \leq Cr^{5/2}.$$

We conclude with the triangle inequality that

$$\|\mathbf{C}(\mathbf{s}) - \Sigma^0(\mathbf{s})\| \leq \|\mathbf{C}(\mathbf{s}) - \Sigma(\mathbf{s})\| + \|\Sigma(\mathbf{s}) - \Sigma^0(\mathbf{s})\| \leq Cr^{5/2}. \quad (52)$$

Again, this holds for any $\mathbf{s} \in S_1$ such that $\|\mathbf{s} - \mathbf{s}^0\| \leq (C_{18} + 1)r$.

Assuming that $\mathbf{s}_i \neq \mathbf{s}^0$ (which is true with probability one) and $\mathbf{s}^0 = 0$, let $h = \|\mathbf{s}_i - \mathbf{s}^0\|$ and $\mathbf{v} = (\mathbf{s}_i - \mathbf{s}^0)/h$. Note that $\mathbf{s}_i = h\mathbf{v}$. Because $\mathbf{v} \perp T_1^0 \cap T_2^0$, and that $\theta_{\min}(T_1^0, T_2^0) \geq \theta_s$, we apply Lemma 20 with scaling to find $\ell \in h \pm r/2$ such that $\|\Sigma^0(\ell\mathbf{v}) - \Sigma^0(h\mathbf{v})\| \geq r^2 C_{20}$, where $C_{20} > 0$ depends only on θ_s and d . Letting $\tilde{\mathbf{s}} = \ell\mathbf{v}$, we have $\|\tilde{\mathbf{s}} - \mathbf{s}_i\| = |h - \ell| \leq r/2$, so that

$$\text{dist}(\tilde{\mathbf{s}}, S_1 \cap S_2) \leq \text{dist}(\mathbf{s}_i, S_1 \cap S_2) + r/2 < (C_{18} + 1/2)r < 1/\kappa,$$

and consequently, $P_{S_1 \cap S_2}(\tilde{\mathbf{s}}) = \mathbf{s}^0$, by (Federer, 1959, Th 4.8(12)). Hence, by the triangle inequality,

$$\begin{aligned} \|\mathbf{C}(\mathbf{s}_i) - \mathbf{C}(\tilde{\mathbf{s}})\| &\geq \|\Sigma^0(\mathbf{s}) - \Sigma^0(\tilde{\mathbf{s}})\| - \|\mathbf{C}(\mathbf{s}_i) - \Sigma^0(\mathbf{s}_i)\| - \|\mathbf{C}(\tilde{\mathbf{s}}) - \Sigma^0(\tilde{\mathbf{s}})\| \\ &\geq r^2/C_{20} - 2Cr^{5/2}. \end{aligned}$$

We apply the same arguments but now coupled with Lemma 19 after applying a proper scaling, to get

$$\begin{aligned}\|C(\bar{\mathbf{s}}) - C(\tilde{\mathbf{s}})\| &\leq \|\Sigma^0(\bar{\mathbf{s}}) - \Sigma^0(\tilde{\mathbf{s}})\| + \|C(\bar{\mathbf{s}}) - \Sigma^0(\bar{\mathbf{s}})\| + \|C(\tilde{\mathbf{s}}) - \Sigma^0(\tilde{\mathbf{s}})\| \\ &\leq 5dr^{3/2}\sqrt{\|\bar{\mathbf{s}} - \tilde{\mathbf{s}}\|} + 2Cr^{5/2},\end{aligned}$$

for any $\bar{\mathbf{s}} \in S_1$ such that $\|\bar{\mathbf{s}} - \tilde{\mathbf{s}}\| \leq r/2$, since this implies that $\|\bar{\mathbf{s}} - \mathbf{s}^0\| \leq (C_{18} + 1)r$. Hence, when $\|\bar{\mathbf{s}} - \tilde{\mathbf{s}}\| \leq r/C_\Omega$ and $r^{1/2} \leq 1/(16CC_{20})$, we have

$$\|C(\bar{\mathbf{s}}) - C(\mathbf{s}_i)\| \geq r^2(1/C_{20} - 5d\sqrt{1/C_\Omega} - 4Cr^{1/2}) \geq r^2/(4C_{20}).$$

Now, under Ω , there is $\mathbf{s}_j \in S_1 \cap B(\bar{\mathbf{s}}, r/C_\Omega)$, so that $\|C_j - C_i\| \geq r^2/(4C_{20})$. Therefore, choosing η such that $\eta < 1/(4C_{20})$, we see that $\|C_j - C_i\| > \eta$, even though $\|\mathbf{s}_j - \mathbf{s}_i\| \leq r/2 + r/C_\Omega \leq r$.

6.2.2 Each cluster forms a connected component in the graph

We show that the points that survive Step 3 and belong to the same cluster form a connected component in the graph, except for possible spurious points near the intersection. Take, for example, the cluster generated from sampling S_1 . The danger is that Step 3 created a ‘‘crevice’’ within this cluster wide enough to disconnect it. We show this is not the case. (Note that the crevice may be made of several disconnected pieces.) Before we start, we recall that I_\star^c was eliminated in Step 3, so that by our choice of η in (50), to show that two points $\mathbf{s}_i, \mathbf{s}_j$ sampled from S_1 are neighbors it suffices to show that $\|\mathbf{s}_i - \mathbf{s}_j\| \leq \varepsilon$.

We first bound the width of the crevice. Let $I_o = \{i \in I_\star : \Xi_i \subset I_\star\}$. By our choice of parameters in (50), we see that $i \in I_o$ is neighbor with any $j \in \Xi_i$, so that i survives Step 3. Hence, the nodes removed at Step 3 are in $I_\dagger := \{i : \Xi_i \cap I_\star^c \neq \emptyset\}$, with the possibility that some nodes in I_\dagger survive. Now, for any $i \notin I_\star$, there is j with $K_j \neq K_i$ such that $\|\mathbf{s}_i - \mathbf{s}_j\| \leq r$, so by Lemma 18,

$$\text{dist}(\mathbf{s}_i, S_1 \cap S_2) \leq C_{18}\|\mathbf{s}_i - \mathbf{s}_j\| \leq C_{18}r.$$

By the triangle inequality, this implies that $\text{dist}(\mathbf{s}_i, S_1 \cap S_2) \leq r_1 := (C_{18} + 1)r$ for all $i \in I_\dagger$. So the crevice is along $S_1 \cap S_2$ and of width bounded by r_1 . We will require that ε is sufficiently larger than r_1 , which intuitive will ensure that the crevice is not wide enough to disconnect the subgraph corresponding to I_o . Let $R := S_1 \setminus B(S_1 \cap S_2, r_2)$, $r_2 = r_1 + r = (C_{18} + 2)r$, so that any $\mathbf{s}_i \in S_1$ such that $\text{dist}(\mathbf{s}_i, R) < r$ survives Step 3.

Take two adjacent connected components of R , denoted R_1 and R_2 . We show that there is at least one pair j_1, j_2 of direct neighbors in the graph such that $\mathbf{s}_{j_m} \in R_m$. Take \mathbf{s} on the connected component of $S_1 \cap S_2$ separating R_1 and R_2 . Let $T^k = T_{S_k}(\mathbf{s})$ and let H be the affine subspace parallel to $(T^1 \cap T^2)^\perp$ passing through \mathbf{s} . Take $\mathbf{t}^m \in P_{T^1}(R_m) \cap H \cap \partial B(\mathbf{s}, \varepsilon_1)$, where $\varepsilon_1 := \varepsilon/2$, and define $\mathbf{s}^m = P_{T^1}^{-1}(\mathbf{t}^m)$. Note that here $\mathbf{t}^1, \mathbf{t}^2 \in T^1$ and $\mathbf{s}^1, \mathbf{s}^2 \in S_1$, and by (Federer, 1959, Th 4.8(12)), $P_{S_1 \cap S_2}(\mathbf{t}^m) = \mathbf{s}$. Lemma 3 not only justifies this construction when $\kappa\varepsilon_1 < 1/3$, it also says that $P_{T^1}^{-1}$ has Lipschitz constant bounded by $1 + \kappa\varepsilon_1$, which implies that

$$\|\mathbf{s}^m - \mathbf{s}\| \leq (1 + \kappa\varepsilon_1)\|\mathbf{t}^m - \mathbf{s}\| = (1 + \kappa\varepsilon_1)\varepsilon_1 \leq \varepsilon/3,$$

when ε is sufficiently small. We also have

$$\begin{aligned}\text{dist}(\mathbf{s}^m, S_1 \cap S_2) &\geq \text{dist}(\mathbf{t}^m, S_1 \cap S_2) - \|\mathbf{s}^m - \mathbf{t}^m\| \\ &= \|\mathbf{t}^m - \mathbf{s}\| - \|\mathbf{s}^m - \mathbf{t}^m\| \\ &\geq \varepsilon_1 - \frac{\kappa}{2}\|\mathbf{s}^m - \mathbf{s}\|^2 \\ &\geq \left(1 - \frac{\kappa}{2}(1 + \kappa\varepsilon_1)^2\varepsilon_1\right)\varepsilon_1 \\ &\geq \varepsilon/3,\end{aligned}$$

when ε is sufficiently small. We used (16) in the second inequality. We assume r/ε is sufficiently small that $\varepsilon/3 \geq r_2 + r$. Then under Ω_1 , there are j_1, j_2 such that $\mathbf{s}_{j_m} \in B(\mathbf{s}^m, r) \cap S_1$. By the triangle inequality, we then have that $\text{dist}(\mathbf{s}_{j_m}, S_1 \cap S_2) \geq \varepsilon/3 - r \geq r_2$, so that $\mathbf{s}_{j_m} \in R_m$, and

$$\begin{aligned} \|\mathbf{s}_{j_1} - \mathbf{s}_{j_2}\| &\leq \|\mathbf{s}_{j_1} - \mathbf{s}^1\| + \|\mathbf{s}^1 - \mathbf{s}\| + \|\mathbf{s} - \mathbf{s}^2\| + \|\mathbf{s}^2 - \mathbf{s}_{j_2}\| \\ &\leq r + \varepsilon/3 + \varepsilon/3 + r \\ &= \frac{2}{3}\varepsilon + 2r \leq \varepsilon, \end{aligned}$$

because $6r \leq 3(r + r_1) \leq \varepsilon$ by assumption.

Now, we show that the points sampled from R_1 form a connected subgraph. (R_1 is any connected component of R .) Take $\mathbf{s}^1, \dots, \mathbf{s}^M$ an r -packing of R_1 , so that

$$\bigcup_m (R_1 \cap B(\mathbf{s}^m, r/2)) \subset R_1 \subset \bigcup_m (R_1 \cap B(\mathbf{s}^m, r)).$$

Because R_1 is connected, $\cup_m B(\mathbf{s}^m, r)$ is necessarily connected. Under Ω_1 , and $C_{22} \geq 2$, all the balls $B(\mathbf{s}^m, r)$, $m = 1, \dots, M$, contain at least one $\mathbf{s}_i \in S_1$, and any such point survives Step 3 since $\text{dist}(\mathbf{s}_i, R_1) < r$ by the triangle inequality. Two points \mathbf{s}_i and \mathbf{s}_j such that $\mathbf{s}_i, \mathbf{s}_j \in B(\mathbf{s}^m, r)$ are connected, since $\|\mathbf{s}_i - \mathbf{s}_j\| \leq 2r \leq \varepsilon$. And when $B(\mathbf{s}^{m_1}, r) \cap B(\mathbf{s}^{m_2}, r) \neq \emptyset$, $\mathbf{s}_i \in B(\mathbf{s}^{m_1}, r)$ and $\mathbf{s}_j \in B(\mathbf{s}^{m_2}, r)$ are such that $\|\mathbf{s}_i - \mathbf{s}_j\| \leq 4r \leq \varepsilon$. Hence, the points sampled from R_1 are connected in the graph under Ω_1 .

We conclude that the nodes corresponding to R that survive Step 3 are connected in the graph.

6.2.3 Choice of parameters

Aside from the constraints displayed in (50), we assumed in addition that

$$r < \frac{1}{C_9\kappa}, \quad r < \frac{1}{C_{18\kappa} + 1}, \quad \eta < \frac{1}{4C_{20}}, \quad 3(C_{18} + 3)r \leq \varepsilon, \quad \varepsilon < \frac{7}{8\kappa},$$

and that ε was sufficiently small. Therefore, it suffices to choose the parameters as in (13) with a large-enough constant.

6.3 Performance guarantees for Algorithm 3

We keep the same notation and go a little faster here as the arguments are parallel. Let d_i denote the estimated dimensionality at point \mathbf{s}_i , meaning the number of eigenvalues of \mathbf{C}_i exceeding $\sqrt{\eta} \|\mathbf{C}_i\|$. Recall that \mathbf{Q}_i denotes the orthogonal projection onto the top d_i eigenvectors of \mathbf{C}_i . The arguments hinge on showing that, under Ω , $d_i = d$ for all $i \in I_\star$ and that $d_i > d$ for i such that $\text{dist}(\mathbf{s}_i, S_1 \cap S_2) \leq r/C$, for some constant $C > 0$.

Take $i \in I_\star$. Under Ω , (43) holds, and applying Weyl's inequality (Stewart and Sun, 1990, Cor. IV.4.9), we have

$$|\beta_m(\mathbf{C}_i) - \beta_m(\boldsymbol{\Sigma}_i)| \leq \zeta r^2, \quad \forall m = 1, \dots, D.$$

By Lemma 11, $\boldsymbol{\Sigma}_i = cr^2 P_{T_i}$, so that $\beta_m(\boldsymbol{\Sigma}_i) = cr^2$ when $m \leq d$ and $\beta_m(\boldsymbol{\Sigma}_i) = 0$ when $m > d$. Hence,

$$\beta_1(\mathbf{C}_i) \leq (c + \zeta)r^2, \quad \beta_d(\mathbf{C}_i) \geq (c - \zeta)r^2, \quad \beta_{d+1}(\mathbf{C}_i) \leq \zeta r^2.$$

This implies that

$$\frac{\beta_d(\mathbf{C}_i)}{\beta_1(\mathbf{C}_i)} \geq \frac{c - \zeta}{c + \zeta} > \sqrt{\eta}, \quad \frac{\beta_{d+1}(\mathbf{C}_i)}{\beta_1(\mathbf{C}_i)} \leq \frac{\zeta}{c + \zeta} < \sqrt{\eta},$$

when $\zeta \leq \eta/2$ as in (50) and η is sufficiently small. When this is so, $d_i = d$ by definition of d_i .

Note that the top d eigenvectors of Σ_i generate T_i . Hence, applying the Davis-Kahan theorem, stated in Lemma 16, and (43) again, we get that

$$\|\mathbf{Q}_i - P_{T_i}\| \leq \frac{\sqrt{2}\zeta r^2}{cr^2} = \zeta' := \sqrt{2}(d+2)\zeta, \quad \forall i \in I_\star.$$

This is the equivalent of (43), which leads to the equivalent of (45):

$$\|\mathbf{Q}_i - \mathbf{Q}_j\| \leq \frac{1}{cr^2} \|\Sigma_i - \Sigma_j\| + 2\zeta', \quad \forall i, j \in I_\star,$$

using the fact that $\Sigma_i = cr^2 P_{T_i}$. When $i, j \in I_\star$ are such that $K_i = K_j$, based on (46), we have

$$\|\mathbf{Q}_i - \mathbf{Q}_j\| \leq 2\kappa\varepsilon + 2\zeta'.$$

Hence, when $\eta > 2\kappa\varepsilon + 2\zeta'$, two nodes $i, j \in I_\star$ such that $K_i = K_j$ and $\|\mathbf{s}_i - \mathbf{s}_j\| \leq \varepsilon$ are neighbors in the graph. The arguments provided in Section 6.2.2 now apply in exactly the same way to show that nodes $i \in I_\star$ such that $K_i = 1$ belong to a single connected component in the graph, except for possible nodes near the intersection. The same is true of nodes $i \in I_\star$ such that $K_i = 2$.

Therefore, it remains to show that these two sets of nodes are not connected. When we take $i, j \in I_\star$ such that $K_i \neq K_j$, we have the equivalent of (49), meaning,

$$\|\mathbf{Q}_i - \mathbf{Q}_j\| \geq \sin \theta_s - 2\kappa(C_{18} + 1)\varepsilon - 2\zeta'.$$

We choose η smaller than the RHS, so that these nodes are not neighbors in the graph.

We next prove that a node $i \in I_\star$ is not neighbor to a node near the intersection because of different estimates for the local dimension. Take $\mathbf{s} \in S_1$ such that $\delta(\mathbf{s}) := \text{dist}(\mathbf{s}, S_2) < r$. We apply Lemma 22 and use the notation there until (53) below, with the exception that we use $\mathbf{s}^2 = P_{S_2}(\mathbf{s})$ and $T_{2(1)}$ to denote $T_{S_2}(\mathbf{s}^2)$. Together with Weyl's inequality, we have

$$\beta_{d+1}(\mathbf{C}(\mathbf{s})) \geq \beta_{d+1}(\Sigma(\mathbf{s})) - C_{22}r^3, \quad \beta_1(\mathbf{C}(\mathbf{s})) \leq \beta_1(\Sigma(\mathbf{s})) + C_{22}r^3,$$

which together with Lemma 21 (and proper scaling), implies that

$$\frac{\beta_{d+1}(\mathbf{C}(\mathbf{s}))}{\beta_1(\mathbf{C}(\mathbf{s}))} \geq \frac{\frac{c}{8}(1 - \cos \theta_{\max}(T_1, T_{2(1)}))^2(1 - (\delta(\mathbf{s})/r)^2)_+^{d/2+1} - C_{22}r^3}{c + (\delta(\mathbf{s})/r)(1 - (\delta(\mathbf{s})/r)^2)_+^{d/2} + C_{22}r^3}.$$

Define \mathbf{s}^0 , T_1^0 and T_2^0 as in Section 6.2.1. Then, by the triangle inequality,

$$\theta_{\max}(T_1, T_{2(1)}) \geq \theta_{\max}(T_1^0, T_2^0) - \theta_{\max}(T_1, T_1^0) - \theta_{\max}(T_{2(1)}, T_2^0).$$

By definition, $\theta_{\max}(T_1^0, T_2^0) \geq \theta_s$, and by Lemma 2,

$$\theta_{\max}(T_1, T_1^0) \leq 2 \operatorname{asin} \left(1 \wedge \frac{\kappa}{2} \|\mathbf{s} - \mathbf{s}^0\| \right) \leq Cr,$$

and similarly,

$$\theta_{\max}(T_{2(1)}, T_2^0) \leq 2 \operatorname{asin} \left(1 \wedge \frac{\kappa}{2} \|\mathbf{s}^2 - \mathbf{s}^0\| \right) \leq Cr,$$

because $\|\mathbf{s} - \mathbf{s}^0\| \leq Cr$ and $\|\mathbf{s}^2 - \mathbf{s}^0\| \leq r + \|\mathbf{s} - \mathbf{s}^0\| \leq Cr$. Hence, for r small enough, $\theta_{\max}(T_1, T_{2(1)}) \geq \theta_s/2$, and furthermore,

$$\frac{\beta_{d+1}(\mathbf{C}(\mathbf{s}))}{\beta_1(\mathbf{C}(\mathbf{s}))} \geq \sqrt{\eta} \quad \text{when} \quad 1 - \frac{\delta(\mathbf{s})^2}{r^2} \geq \xi^{2/(d+2)}, \quad (53)$$

where

$$\xi := \frac{9(1+1/c)\sqrt{\eta}}{(1-\cos(\theta_s/2))^2},$$

by the fact that $\eta \geq r$ in (50). The same is true for points on $\mathbf{s} \in S_2$ if we redefine $\delta(\mathbf{s}) = \text{dist}(\mathbf{s}, S_1)$. Hence, for \mathbf{s}_i close enough to the intersection that $\delta(\mathbf{s}_i)$ satisfies (53), $d_i > d$. Then, by Lemma 15, $\|\mathbf{Q}_i - \mathbf{Q}_j\| = 1$ for any $j \in I_*$. By our choice of $\eta < 1$, this means that i and j are not neighbors.

So the only way $\{i \in I_* : K_i = 1\}$ and $\{i \in I_* : K_i = 2\}$ are connected in the graph is if there are $\mathbf{s}_i \in S_1$ and $\mathbf{s}_j \in S_2$ such that $\|\mathbf{s}_i - \mathbf{s}_j\| \leq \varepsilon$ and both $\delta(\mathbf{s}_i)$ and $\delta(\mathbf{s}_j)$ fail to satisfy (53). We now show this is not possible. By Lemma 22, we have

$$\|\mathbf{C}_i - \boldsymbol{\Sigma}_i\| \leq C_{22} r^3.$$

By (39) (and using the corresponding notation) and the triangle inequality

$$\begin{aligned} \|\boldsymbol{\Sigma}_i - \alpha_i c r^2 P_{T_i}\| &\leq c(1-\alpha_i)t_i^2 r^2 + \alpha_i(1-\alpha_i)\delta^2(\mathbf{s}_i) \leq 2(1-\alpha_i)r^2 \\ &\leq 2(1-(\delta(\mathbf{s}_i)/r)^2)_+^{d/2} r^2 \leq 2\xi^{d/(d+2)} r^2, \end{aligned}$$

where the very last inequality comes from $\delta(\mathbf{s}_i)$ not satisfying (53). Hence,

$$\|\mathbf{C}_i - \alpha_i c r^2 P_{T_i}\| \leq 2\xi^{d/(d+2)} r^2 + C_{22} r^3,$$

and since the $\beta_{d+1}(P_{T_i}) = 0$, by the Davis-Kahan theorem, we have

$$\|\mathbf{Q}_i - P_{T_i}\| \leq \frac{1}{\alpha_i c r^2} [\xi^{d/(d+2)} r^2 + C_{22} r^3] \leq C(\xi^{d/(d+2)} + r),$$

and similarly,

$$\|\mathbf{Q}_j - P_{T_j}\| \leq C(\xi^{d/(d+2)} + r).$$

By Lemma 15, $\|P_{T_i} - P_{T_j}\| = \sin \theta_{\max}(T_i, T_j)$. Let $\mathbf{s}^0 = P_{S_1 \cap S_2}(\mathbf{s}_i)$, and define T_1^0 and T_2^0 as before. We have

$$\theta_{\max}(T_i, T_j) \geq \theta_{\max}(T_1^0, T_2^0) - \theta_{\max}(T_i, T_1^0) - \theta_{\max}(T_j, T_2^0) \geq \theta_s - C\varepsilon,$$

calling in Lemma 2 as before, coupled with the fact that $\|\mathbf{s}_i - \mathbf{s}^0\| \leq C\varepsilon$ and $\|\mathbf{s}_j - \mathbf{s}^0\| \leq C\varepsilon$, since $\text{dist}(\mathbf{s}_i, S_2) \leq \|\mathbf{s}_i - \mathbf{s}_j\| \leq \varepsilon$ and Lemma 18 applies, and then $\|\mathbf{s}_j - \mathbf{s}^0\| \leq \|\mathbf{s}_i - \mathbf{s}^0\| + \|\mathbf{s}_j - \mathbf{s}_i\|$. Hence, assuming ε is small enough,

$$\begin{aligned} \|\mathbf{Q}_i - \mathbf{Q}_j\| &\geq \|P_{T_i} - P_{T_j}\| - \|\mathbf{Q}_i - P_{T_i}\| - \|\mathbf{Q}_j - P_{T_j}\| \\ &\geq \sin(\theta_s/2) - C(\xi^{d/(d+2)} + r) > \eta, \end{aligned}$$

when r and η (and therefore ξ) are small enough. Therefore i and j are not neighbors, as we needed to show.

We conclude by remarking that, by choosing C large enough in (13), the resulting choice of parameters fits all our (often implicit) requirements.

6.4 Noisy case

So far we only dealt with the case where $\tau = 0$ in (11). When $\tau > 0$, a sample point \mathbf{x}_i is in general different than its corresponding point \mathbf{s}_i sampled from one of the surfaces. However, when τ/r is small, this does not change things much. For one thing, the points are close to each other, since we have $\|\mathbf{x}_i - \mathbf{s}_i\| \leq \tau$ by assumption, and τ is small compared to r . And the corresponding covariance

matrices are also close to each other. To see this, redefine $\Xi_i = \{j \neq i : \mathbf{x}_j \in N_r(\mathbf{x}_i)\}$ and \mathbf{C}_i as the sample covariance of $\{\mathbf{x}_j : j \in \Xi_i\}$. Let \mathbf{D}_i denote the sample covariance of $\{\mathbf{s}_j : j \in \Xi_i\}$. Let X be uniform over $\{\mathbf{x}_j : j \in \Xi_i\}$ and define $Y = \sum_j \mathbf{s}_j \mathbb{I}_{\{X=\mathbf{x}_j\}}$. As in (24), we have

$$\begin{aligned} \|\mathbf{D}_i - \mathbf{C}_i\| &= \|\text{Cov}(X) - \text{Cov}(Y)\| \\ &\leq \mathbb{E} [\|X - Y\|^2]^{1/2} \cdot \left(\mathbb{E} [\|X - \mathbf{x}_i\|^2]^{1/2} + \mathbb{E} [\|Y - \mathbf{x}_i\|^2]^{1/2} \right) \\ &\leq \tau \cdot (r + r + \tau) = r^2(2\tau/r + (\tau/r)^2), \end{aligned} \tag{54}$$

which is small compared to r^2 , which is the operating scale for covariance matrices in our setting.

Using these facts, the arguments are virtually the same, except for some additional terms due to triangle inequalities, for example, $\|\mathbf{s}_i - \mathbf{s}_j\| - 2\tau \leq \|\mathbf{x}_i - \mathbf{x}_j\| \leq \|\mathbf{s}_i - \mathbf{s}_j\| + 2\tau$. In particular, this results in ζ in (44) being now redefined as $\zeta = \frac{3\tau}{r} + t + C_{13}\kappa r$. We omit further technical details.

Acknowledgements

We would like to thank Jan Rataj for hints leading to Lemma 2, which is much sharper than what we knew from (Niyogi et al., 2008). We would also like to acknowledge support from the Institute for Mathematics and its Applications (IMA). For one thing, the authors first learned about the research of Goldberg et al. (2009) there, at the *Multi-Manifold Data Modeling and Applications* workshop in the Fall of 2008, and this was the main inspiration for our paper. Also, part of our work was performed while TZ was a postdoctoral fellow at the IMA, and also while EAC and GL were visiting the IMA. This work was partially supported by grants from the National Science Foundation (DMS-09-15160, DMS-09-15064, DMS-09-56072).

References

- Afriat, S. N. (1957). Orthogonal and oblique projectors and the characteristics of pairs of vector spaces. *Proc. Cambridge Philos. Soc.* 53, 800–816.
- Agarwal, S., K. Branson, and S. Belongie (2006). Higher order learning with graphs. In *ICML*, pp. 17–24.
- Agarwal, S., J. Lim, L. Zelnik-Manor, P. Perona, D. Kriegman, and S. Belongie (2005). Beyond pairwise clustering. In *CVPR*, pp. 838–845.
- Arias-Castro, E. (2011). Clustering based on pairwise distances when the data is of mixed dimensions. *Information Theory, IEEE Transactions on* 57(3), 1692–1706.
- Arias-Castro, E., G. Chen, and G. Lerman (2011). Spectral clustering based on local linear approximations. *Electron. J. Statist.* 5, 1537–1587.
- Basri, R. and D. Jacobs (2003). Lambertian reflectance and linear subspaces. *IEEE PAMI* 25(2), 218–233.
- Bradley, P., K. Bennett, and A. Demiriz (2000). Constrained k -means clustering. Technical Report MSR-TR-2000-65, Microsoft Research.
- Brito, M. R., E. L. Chávez, A. J. Quiroz, and J. E. Yukich (1997, August). Connectivity of the mutual k -nearest-neighbor graph in clustering and outlier detection. *Statistics & Probability Letters* 35(1), 33–42.
- Chen, G., S. Atev, and G. Lerman (2009). Kernel spectral curvature clustering (KSCC). In *ICCV Workshops*, Kyoto, Japan, pp. 765–772.
- Chen, G. and G. Lerman (2009a). Foundations of a multi-way spectral clustering framework for hybrid linear modeling. *FOCM* 9(5), 517–558.

- Chen, G. and G. Lerman (2009b). Spectral curvature clustering (SCC). *IJCV* 81(3), 317–330.
- Davis, C. and W. M. Kahan (1970). The rotation of eigenvectors by a perturbation. III. *SIAM J. Numer. Anal.* 7, 1–46.
- Elhamifar, E. and R. Vidal (2011). Sparse manifold clustering and embedding. In J. Shawe-Taylor, R. Zemel, P. Bartlett, F. Pereira, and K. Weinberger (Eds.), *Advances in Neural Information Processing Systems 24*, pp. 55–63.
- Epstein, R., P. Hallinan, and A. Yuille (1995, June). 5 ± 2 eigenimages suffice: An empirical investigation of low-dimensional lighting models. In *IEEE Workshop on Physics-based Modeling in Computer Vision*, pp. 108–116.
- Federer, H. (1959). Curvature measures. *Trans. Amer. Math. Soc.* 93, 418–491.
- Fu, Z., W. Hu, and T. Tan (2005). Similarity based vehicle trajectory clustering and anomaly detection. In *ICIP*, pp. II–602–5.
- Gionis, A., A. Hinneburg, S. Papadimitriou, and P. Tsaparas (2005). Dimension induced clustering. In *KDD '05: Proceedings of the eleventh ACM SIGKDD international conference on Knowledge discovery in data mining*, New York, NY, USA, pp. 51–60. ACM.
- Goldberg, A., X. Zhu, A. Singh, Z. Xu, and R. Nowak (2009). Multi-manifold semi-supervised learning. In *AISTATS*, pp. 169–176.
- Gong, D., X. Zhao, and G. Medioni (2012, July). Robust multiple manifolds structure learning. In J. Langford and J. Pineau (Eds.), *Proceedings of the 29th International Conference on Machine Learning (ICML-12)*, ICML '12, New York, NY, USA, pp. 321–328. Omnipress.
- Guo, Q., H. Li, W. Chen, I.-F. Shen, and J. Parkkinen (2007). Manifold clustering via energy minimization. In *ICMLA '07: Proceedings of the Sixth International Conference on Machine Learning and Applications*, Washington, DC, USA, pp. 375–380. IEEE Computer Society.
- Haro, G., G. Randall, and G. Sapiro (2007). Stratification learning: Detecting mixed density and dimensionality in high dimensional point clouds. *Advances in Neural Information Processing Systems 19*, 553.
- Ho, J., M. Yang, J. Lim, K. Lee, and D. Kriegman (2003). Clustering appearances of objects under varying illumination conditions. In *CVPR*, pp. 11–18.
- Hoeffding, W. (1963). Probability inequalities for sums of bounded random variables. *J. Amer. Statist. Assoc.* 58, 13–30.
- Kaslovsy, D. N. and F. G. Meyer (2011). Optimal tangent plane recovery from noisy manifold samples. *CoRR abs/1111.4601*.
- Kushnir, D., M. Galun, and A. Brandt (2006). Fast multiscale clustering and manifold identification. *Pattern Recogn.* 39(10), 1876–1891.
- Little, A., Y. Jung, and M. Maggioni (2009). Multiscale estimation of intrinsic dimensionality of data sets. In *Manifold learning and its applications.*, AAAI Fall Symposium Series, pp. 26–33.
- Luxburg, U. (2007). A tutorial on spectral clustering. *Statistics and Computing* 17(4), 395–416.
- Ma, Y., A. Y. Yang, H. Derksen, and R. Fossum (2008). Estimation of subspace arrangements with applications in modeling and segmenting mixed data. *SIAM Review* 50(3), 413–458.
- Maier, M., M. Hein, and U. von Luxburg (2009). Optimal construction of k-nearest-neighbor graphs for identifying noisy clusters. *Theor. Comput. Sci.* 410(19), 1749–1764.
- Martínez, V. and E. Saar (2002). *Statistics of the Galaxy Distribution*. Boca Raton: CRC press.
- Ng, A., M. Jordan, and Y. Weiss (2002). On spectral clustering: Analysis and an algorithm. *Advances in neural information processing systems 2*, 849–856.
- Niyogi, P., S. Smale, and S. Weinberger (2008). Finding the homology of submanifolds with high confidence from random samples. *Discrete Comput. Geom.* 39(1), 419–441.
- Polito, M. and P. Perona (2001). Grouping and dimensionality reduction by locally linear embedding. *Advances in Neural Information Processing Systems 14*, 1255–1262.

- Shashua, A., R. Zass, and T. Hazan (2006). Multi-way clustering using super-symmetric non-negative tensor factorization. In *ECCV*, pp. 595–608.
- Soltanolkotabi, M. and E. J. Candès (2011). A geometric analysis of subspace clustering with outliers. *CoRR abs/1112.4258*.
- Souvenir, R. and R. Pless (2005). Manifold clustering. In *Computer Vision, 2005. ICCV 2005. Tenth IEEE International Conference on*, Volume 1, pp. 648–653 Vol. 1.
- Stewart, G. W. and J. G. Sun (1990). *Matrix perturbation theory*. Computer Science and Scientific Computing. Boston, MA: Academic Press Inc.
- Tipping, M. and C. Bishop (1999). Mixtures of probabilistic principal component analysers. *Neural Computation* 11(2), 443–482.
- Tropp, J. (2012). User-friendly tail bounds for sums of random matrices. *Foundations of Computational Mathematics* 12, 389–434.
- Valdarnini, R. (2001). Detection of non-random patterns in cosmological gravitational clustering. *Astronomy & Astrophysics* 366, 376–386.
- Vidal, R. and Y. Ma (2006). A unified algebraic approach to 2-D and 3-D motion segmentation and estimation. *JMIV* 25(3), 403–421.
- Walther, G. (1997). Granulometric smoothing. *Ann. Statist.* 25(6), 2273–2299.
- Wang, Y., Y. Jiang, Y. Wu, and Z.-H. Zhou (2011, july). Spectral clustering on multiple manifolds. *Neural Networks, IEEE Transactions on* 22(7), 1149–1161.
- Zelnik-Manor, L. and P. Perona (2004). Self-tuning spectral clustering. In *NIPS*, pp. 1601–1608.
- Zhang, T., A. Szlam, Y. Wang, and G. Lerman (2012). Hybrid linear modeling via local best-fit flats. *International Journal of Computer Vision*, 1–24.